



UPPSALA  
UNIVERSITET

ES14045

Examensarbete 30 hp  
Februari 2015

# Dynamic positioning of a semi- submersible, multi-turbine wind power platform

---

John Ayotte



UPPSALA  
UNIVERSITET

Teknik- naturvetenskaplig fakultet  
UTH-enheten

Besöksadress:  
Ångströmlaboratoriet  
Lägerhyddsvägen 1  
Hus 4, Plan 0

Postadress:  
Box 536  
751 21 Uppsala

Telefon:  
018 - 471 30 03

Telefax:  
018 - 471 30 00

Hemsida:  
<http://www.teknat.uu.se/student>

## Abstract

### **Dynamic positioning of a semi-submersible, multi-turbine wind power platform**

*John Ayotte*

As a growing market for offshore wind power has created a niche for deep-water installations, offshore floating wind solutions have become more and more viable as a renewable energy source. This technology is currently in development and as with many new technologies, many traditional design methods are found lacking. In the multi-turbine platform design investigated, turbine units are placed closely together to conserve material use and reduce cost, however with such tightly spaced turbines; wake interaction poses a threat to the productivity and the lifespan of the installation. In order to fully capitalize on the substantial increase in available wind energy far at sea, it is important that these floating parks operate in an optimal way. The platform investigated in this report sports 3, 6MW turbines which must be positioned such that wake interference is minimized; the platform must always bear a windward heading.

Maneuvering ocean going vessels has been practiced using automated dynamic positioning systems in the gas and oil industry for over 50 years, often employing submerged thrusters as a source of propulsion. These systems are mostly diesel powered and require extra operational maintenance, which would otherwise increase the cost and complexity of a floating wind farm. In this paper, it is suggested that the wind turbines themselves may be used to provide the thrust needed to correct the platform heading, thus eliminating the practical need for submerged thrusters. By controlling the blade pitch of the wind turbines, a turning moment (torque) can be exerted on the platform to correct heading (yaw) relative wind direction. Using the Hexicon H3-18MW platform as a starting point; hydrodynamic, aerodynamic and electromechanical properties of the system are explored, modeled and attempts at model predictive control are made. Preliminary results show that it is possible to control the H3's position (in yaw) relative the wind using this novel method.

Handledare: John Holm  
Ämnesgranskare: Bengt Carlsson, Alexander Medvedev  
Examinator: Petra Jönsson  
ISSN: 1650-8300, UPTec ES14 045

## **Executive Summary**

This report looks at modeling the Hexicon H3-18MW platform and controlling the platform's yaw relative to the wind using the turbine blade pitch as a source of thrust. The hydrodynamics of the platform are described using the Morison equations, as well as the H3-18MW specific geometry and layout. The scaled NREL-6MW turbine is used for reference throughout this work. While many of the turbine's specifications are available through open source channels, new information describing the turbine tip speed ratio at sub-optimal blade pitch settings was calculated using the FEM program ASHES. The Jensen wake model is used to explain wake behavior. The many models are combined in several MATLAB scripts to create a platform simulator from which multi-input, multi-output models are approximated in a black box fashion. Results show that the H3-18MW platform is controllable in yaw using the collective control technique, wholly through the manipulation of turbine blade pitch. Future work should include a more white-box approach to the modeling steps, hopefully resulting in more accurate and reliable models. Likewise, the model predictive controller designed for this project should be revisited as SIMULINK software is updated.

## Populärvetenskaplig sammanfattning

Den växande efterfrågan av förnybara energikällor, både från myndigheter och från konsumenter har skapat en marknad för havsbaserad vindkraft. Nuvarande teknik för konstruktioner av vindkraftsfundament begränsas till grundare vatten. Med tanke på att vindarna är starkare och mer förutsägbara långt ut till havs finns ett behov av utveckling av flytande djuphavsinstallationer där vindkraftverk kan producera el utan att stå på bottenfundament.

Flytande plattformsteknik för vindkraft är fortfarande under utveckling. I denna rapport undersöks en flytande multiturbinsplattform utvecklad av det svenska vindkraftsföretaget Hexicon AB. För att göra investering i havsbaserad vindkraft ekonomisk och miljömässigt försvarbar krävs att plattformen är billig och kompakt i förhållande till producerad el, detta innebär att vindturbinerna placeras relativt tätt på Hexicons plattformar. En mindre plattform innebär en förenklad byggnation, mindre materialåtgång samt mindre underhåll. Nackdelar med en kompakt plattform är att närstående turbiner medför risk för turbinvakinterferens, det vill säga att turbinerna skuggar varandra så att en turbin hamnar i lä bakom en annan. Detta leder till produktionsbortfall och i värsta fall kan minska livslängden på turbinerna. För att motverka vakinterferensen måste plattformar av denna typ vridas så att turbinerna står riktade hela tiden i den ostörda vindens riktning.

Dynamiska positioneringssystem är en teknik som används för att kontrollera och styra de allra största sjöfartygen, främst inom den havsbaserade oljeindustrin, för att dessa stora fartyg ska ligga rätt i vattnet och minska slitaget från vind och vågor. Fartygen vrids oftast i rätt riktning med hjälp av bogpropellrar. Dessa system kräver en hel del underhåll och är dessutom beroende av diesel eller annat bränsle. Ett dieseldrivet system skulle försvåra konstruktionen och underhållet av flytande vindkraftsplattformar och försämra en annars grön energikälla. I denna rapport utforskas möjligheten att styra plattformen med kraft som naturligt utvecklas i vindturbinerna genom manipuleringen av turbinbladsvinkeln. Om en sådan lösning är möjligt skulle det förbättra produktiviteten, eliminera behovet av bogpropellrar och ytterligare förenkla konstruktionen av plattformen.

I detta arbete är Hexicon AB:s H3-18MW multiturbinsplattform modellerat ur en aerodynamisk, hydrodynamisk, och elektromekanisk perspektiv. Från modellerna skapas en H3-18MW-simulator i MATLAB. Från simuleringens syntetiska in- och utdata approximeras linjära multi-input, multi-output modeller som regleras med en logisk regulator i SIMULINK. Det preliminära resultatet visar att det är möjligt att styra plattformen med avseende på girningen mot vinden. Vidare diskuteras möjligheter och fördelarna med denna typ av kollektivkontroll av vindkraftsparker i stort.

# Contents

Executive Summary .....	3
Populärvetenskaplig sammanfattning .....	4
Acknowledgements .....	7
Glossary of terms, acronyms and symbols .....	7
1 Introduction .....	8
2 Background .....	10
2.1 Offshore wind power .....	10
2.1.1 Common methods and disadvantages .....	10
2.2 Floating platforms in general .....	13
2.3 The Hexicon solution .....	16
2.4 Dynamic positioning .....	19
2.4.1 DP for the control of the Hexicon H3-18MW platform .....	21
3 Theory .....	23
3.1 Hydrodynamic theory .....	23
3.2 Turbine theory .....	27
3.3 Wake theory .....	28
3.4 System identification .....	30
3.5 Model predictive control .....	32
4 Method .....	35
4.1 Modeling in general .....	35
4.2 Linear model approximation .....	37
4.3 Control with SIMULINK model .....	39
5 Results .....	41
5.1 Platform models .....	41
5.1.1 Hydrodynamic model .....	41
5.1.2 Aerodynamic models; wake and blade behavior .....	42
5.1.3 Electro-mechanical models .....	50
5.2 System identification .....	55
5.3 System control .....	63
6 Sensitivity Analysis .....	72

7 Discussion .....	74
8 Conclusions.....	77
8.1 Modeling.....	77
8.2 System identification .....	77
8.3 Systems control.....	77
9 Future works.....	79
Bibliography.....	81
Appendix .....	85

## **Acknowledgements**

*This paper is dedicated to my family, and though many of them are on the far side of the world, my thoughts are with them.*

*In addition to the dedication, I would like to acknowledge and give my sincerest acclamation of gratitude to some of the many fine people who have helped me along the way. Thank you to Professor Bengt Carlsson, John Holm, Niklas Hummel, Filipe Rebello, Rubén Cubo and Professor Alexander Medvedev along with all my friends and family who listened patiently these last five months.*

## **Glossary of terms, acronyms and symbols**

MATLAB – engineering software used for calculations

SIMULINK – MATLAB based simulation software

HAWTs- Horizontal axis wind turbines, specifically upwind, active pitch controlled turbines.

OWP- Offshore wind power

OFP- Offshore floating platform

DOF(s) – degree(s) of freedom

NREL- National Renewable Energy Laboratory responsible for the NREL reference turbine,

P- Power [W]

T- Thrust [Nm]

A - Turbine (swept) rotor area in [m<sup>2</sup>]

$\rho$  - Density of fluid in [kg/m<sup>3</sup>]. Used for both air and sea water in report.

$C_p$  - Power coefficient of turbine

$C_t$  – Thrust coefficient of turbine

$\lambda$  - Tip speed ratio (see TSR)

TSR – Tip speed ratio (see  $\lambda$ )

PM – Position mooring

PID – Proportional-integral-derivative controller

MPC – Model predictive control (see section dealing with model predictive control)

PRBS- Pseudo random binary signal used as a system input in system identification problems.

BLA- Best linear approximation

IDENT- MATLAB's system identification toolbox

Bang-bang – A simple feedback controller which switches between two states. In this report the modified bang-bang controller switches between the upper and lower pitch boundary as determined by the wind speed.

## **1 Introduction**



In this report, a novel method for actively controlling the yaw of a semi-submersible, multi-turbine wind power platform is developed and investigated. The Hexicon AB platform model H3-18MW is used for the basis of this investigation. The turbines and platform are modeled using known and calculated physical information. From these models, a state space representation is estimated from synthetic simulated data and incorporated into a model predictive (MPC) controller.

The blade pitch of the individual turbines is manipulated, changing the individual turbine thrust and creating a turning moment (torque) on the platform. This turning moment can be controlled to direct the platform into the oncoming wind. While most modern forms of dynamic positioning (DP) are performed via control of submerged thrusters, this project attempts to choreograph yawing maneuvers solely using the blade pitch angle on a group of horizontal axis wind turbines (HAWTs). A scaled NREL 6MW turbine, based on the open source 5MW NREL turbine is used to represent a generic HAWT.

This paper is presented first with a background, outlining the benefits and challenges of offshore wind power, and how these problems may be rectified with floating offshore wind parks. Following background information, the theory used in this work is presented. The theory section can be read as a stand-alone guide and equations derived here are referred to throughout the work. A shorter ‘methods’ section outlines the tools and software used to create the models and run simulations and the results of the project follow. Lastly, conclusions, a discussion of these conclusions and suggestions for future work with this project are presented. Attempts have been made to provide continuity for the reader, in all sections, the three major themes of systems modeling, linear systems approximation and systems control presented in order.

## **2 Background**

### **2.1 Offshore wind power**

Offshore wind power (OWP) has many significant advantages over land based wind energy which has led to a growing interest in the field of OWP over the last 3 decades. From the early 90's offshore installed capacity has grown from nearly nothing to a present global installed capacity of nearly 35,000 MW (Erlich et al., 2013: 891). Apart from the technical advantages, which are addressed below, current market research has found that OWP has a greater level of public acceptability when compared to land based wind power, as the visibility of the turbines and experienced noise and flicker levels are reduced (Ladenburg, 2008:111), (Miller et al. 2007:814) (Heidelberg, 2006:615-652).

Due to the lack of physical barriers (forests, mountains, buildings etc.), the winds at sea are in general stronger, more consistent (in terms of heading and speed) and contain lower levels of turbulence than winds measured over land (Adelaja, 2011:191), (Esteban et al. 2011:444). These factors allow for greater production levels, a higher level of availability, and a reduced stochastic loading due to reduced turbulence. This can lead to an increase in the lifespan of the turbines (Esteban et al. 2011:444). While building and installing wind turbines at sea does present technical difficulties above and beyond those met with onshore constructions, the global offshore wind resource is estimated to be much greater (around 37,000 TWh/year) than the global land based wind resource (13,000 TWh/y) which has led to growing interest in within the field (Esteban et al. 2011:444).

#### **2.1.1 Common methods and disadvantages**

Due to the limitations of existing construction techniques, the placement of offshore wind turbines is generally confined to water depths between 0 and 40 meters. While techniques exist that allow greater depths, the average depth of OWP turbines is closer to 23 meters (EWEA, 2012:16).

Given these critical depth and distance limitations, many of the described advantages of OWP are reduced significantly as wind conditions nearer shore are ultimately inferior to deep water conditions. In order to gain access to the 30-40% increase in wind energy content experienced in 'open seas', a minimum offshore distance of 10-100 km is usually necessary (Heidelberg, 2006:615-652). The following plot (Figure 1) shows the 2011 European offshore wind installations as a function of water depth and distance to shore. While several deeper sea projects are consented to, the overall majority of online projects are found in shallow water (less than 30 meters) in near shore areas (less than 30 km) areas.

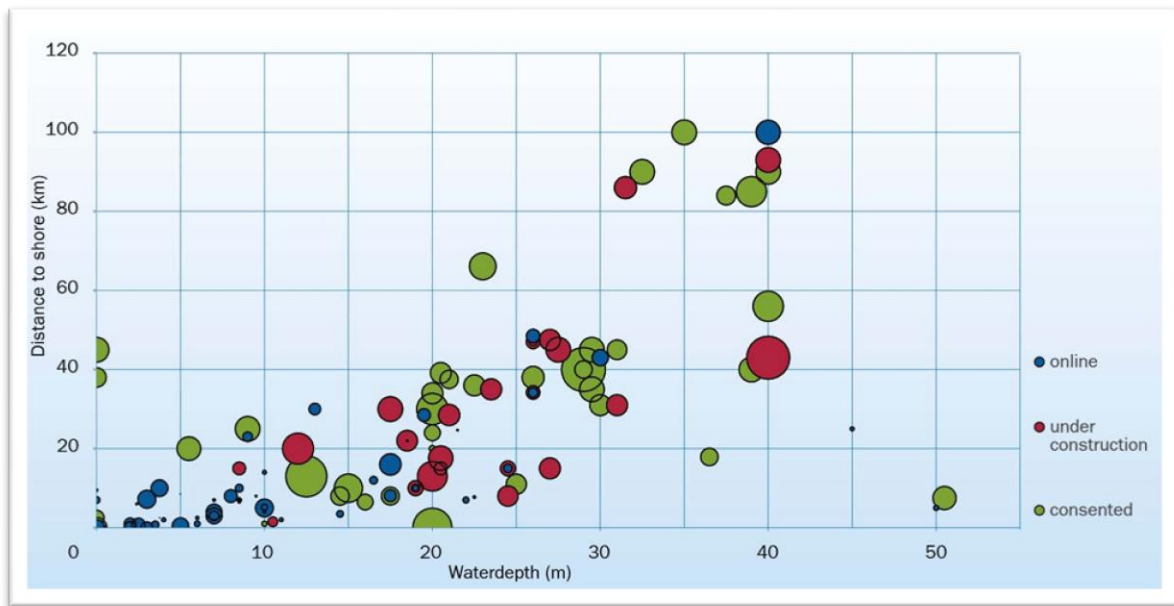


Figure 1 EWEA, 2013 plot of current and planned offshore projects. A clear trend towards deeper, more distant installations reflects the potential increase in power production far at sea.

As Heidelberg states in his chapter on ‘technology of offshore siting’ “...the most far reaching adaptation demanded by offshore siting is associated with the tower design and its foundation on the sea floor” (Heidelberg, 2007:615-652). This is due to increased complexity of offshore foundations and the methods used to construct them, as water depth plays a critical role in choice of technology. Common methods can be seen in Table 1, showing method as a function of water depth.

Table 1 while some techniques allow depths of up to 60 meters, the average water depth of installed turbines around the world as of 2011 is roughly 23 meters. Figure data collected from Heidelberg 2007.

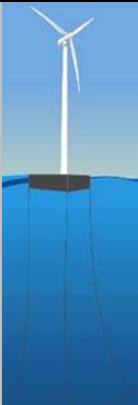

Method	Description/points of interest	Depth [m]	limits
<b>Monopile</b>	Sea bed must consist of sand or gravel	0 -25	
<b>Gravity base</b>	Most cost effective solution in shallow water	0-60	
<b>Tripod piled structure</b>	Used where sea floor is uneven, high stability	0-60	
<b>floating</b>	Anchored with mooring line(s)	40-400	

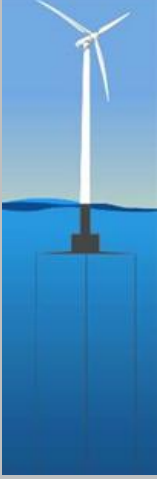
A combination of the methods described above can be required for use in a single site pending the specific water depth and seafloor composition. This places a greater demand on specialized OWP construction equipment, such as jack up boats and purpose built construction vessels (Heidelberg, 2007:615-652). Offshore floating platforms (OFPs) though still in a developmental phase, could allow for more optimal siting and greater access to promising offshore wind resources. Furthermore, because OFPs are not limited by the sub-sea terrain or water depth, a greater flexibility in construction methods (available support and construction vessels) is allowed (Roddier et al., 2010:1).

## 2.2 Floating platforms in general

The concept of OFPs finds its roots in 1972, first postulated by Professor William Heronemus at the University of Massachusetts. However, it was not before the 1990's that OFPs gained traction as a viable alternative to traditional (foundation based) OWP turbines. Since then the field has opened up to a multitude of design variations, the overwhelming majority of which focusing on single turbine platforms (Butterfield et al., 2007:8). The principal design methods can be seen in Table 2 below.

Table 2 showing an overview of the three main floating platform types which can be used to support offshore wind turbines. The type of platform chosen depends on the depth of mooring and local bottom conditions.

Image	Type	Description/method	Notable
	Semi-submersible platform, also called buoyancy platform	Achieves stability much in the same way as a barge- through the stabilizing moment of the weighted water plane.	Flexible mooring solutions available depending on depth and demands on mobility.
	Spar platform	Gains stability through an extended, weighted/ballast foundation (also known as ballast platform). When moored, the platform stands vertically in the water.	Due to extended foundation, this platform type is not always practical in more shallow waters.

	<b>Tension leg platform</b> (TLP)	Uses several mooring lines (under tension) which hold the platform, floating in place near the surface.	Due to high stiffness in 'legs' and need for several points of connection with the ocean floor, movement is restricted. Suitable for single turbine platforms.
---	-----------------------------------	---	--

All three methods use mooring lines in one way or another to limit the motion of a turbine platform and anchor it to the sea floor (Butterfield et al., 2007:6). According to various authors each of these OFPs could be deployed in deep water environments and provide cost competitive OWP solutions (Butterfield et al., 2007:7). The mooring method used however is highly dependent on water depth as seen in Table 3 below.

Table 3 describing conventional mooring solutions as a function of depth (Hexicon, 2014)

**Mooring line solutions available for OFPs**

Type	Depth [m]	Description
<b>Shallow water chain system</b>	40-60	Simple chain construction linking platform with sea floor
<b>Chain catenary system</b>	40-100	Most commonly used, several chains lie horizontal on seabed, arching upwards to platform connection.
<b>Wire/rope mooring</b>	> 100	High elasticity needed at greater depths, synthetic rope used instead of wires at depths greater than 2000 meters.

Despite the method used, the H3-platform is free to rotate about the central hub giving free rotation in the surge sway plane.

While the use of OFPs for wind power generation is still in its infancy, several floating projects are currently online and delivering electricity to the grid and many more novel concepts exist (see Table 4). The following is a brief overview of some of the existing OFP solutions:

**Table 4** Compiled statistics from (BlueHgroup, 2010) (StatOil, 2012) (Windfloat, 2014) (Dagher, 2013) (GICON, 2014)

<b>Concept name</b>	<b>Brief description</b>	<b>Status</b>
<b>Blue Technologies, Netherlands</b>	<b>H</b> Tension leg platform with single- two bladed HAWT	Working 80 kW prototype (2008), Currently seeking finance for full scale (5MW) project. (Bluehgroup)
<b>Hywind Project (StatOil) Norway</b>	Ballast stabilized with single- 3 bladed HAWT	2.3 MW prototype online since 2009.
<b>Windfloat pacific, Oregon, USA.</b>	Semi-submersible platform with single- 3 bladed HAWT	Planned 30 MW park of 5 individual windfloat platforms. Est completion by 2017.
<b>VoltturnUS, University of Maine, USA</b>	Semi-submersible platform with single- 3 bladed HAWT	Deployed and grid connected in 2013.
<b>GiCon, Hamburg, Germany</b>	Tension leg platform, single- 3 bladed HAWT	Scale model testing complete as of 2012. Full scale prototype under construction as of 2014.
<b>Fukushima, Fukushima offshore wind consortium</b>	Semi-submersible and spar style platform concepts. Single 3-bladed HAWT turbines.	Scale testing and plans to erect 6, 2MW platforms by 2016, up to 80 2MW platforms by 2020 pending success of initial installation.

### **2.3 The Hexicon solution**

Hexicon AB is a Swedish, Stockholm based company that started in 2009 with the aim of designing and constructing semi-submersible, multi turbine wind power platforms for offshore energy production. A semi-submersible platform is a buoyancy type platform long since used in the offshore oil industry as a drilling vessel (Journée, et al., 2001:256). Though several models of the Hexicon design exist, in principle each platform is similar in composition. The main platform consists of a lattice style structure built of slender, cylindrical, steel beams, and in each node of the platform, sits an offshore wind turbine. All the sections are connected with lattice framework around a central turret, which also acts as the mooring point for the entire structure (see Figure 2 and/or Figure 3). Unlike the majority of OFPs, all Hexicon platform models supports several turbines. This is done in order to reduce the overall cost of the park as each turbine is effectively sharing platform space. Moreover, with many turbines on one platform the turbines can be connected together electrically within the platform. In traditional OWP parks each turbine is electrically connected to neighboring turbines via sea cables. Attempts are made at optimizing park layout early on in site development to reduce the amount of material used as much as possible as sea cables stand on average for 2% of a given OWP park's levelized cost of energy (Arwas et al., 2012:22). The Hexicon concept effectively removes the need for sea cable linkage between turbines, instead cheaper cables can be used as they are protected within the platform structure.

Like other OFPs the Hexicon platform can be moored at great depths, allowing heightened flexibility when siting the park. The central turret mooring allows the entire platform to yaw freely into the wind at all times. In theory the platform is always positioned to face the wind, effectively avoiding wake interaction. This means the turbines may be placed closer together, hopefully minimizing material costs and simplifying overall design.

Wake interaction, or wake loss is a phenomena that occurs when a turbine stands in the downstream wake of another turbine leading to a loss in wind power capture, and an increase in loads. In traditional wind power parks this phenomenon has been widely researched and methods for reducing wake loss are employed in smart wind farm layout design (Song, 2009:685), (Grady et al., 2005:259). As a rule of thumb it can be said that (fixed foundation) wind turbines should be placed "... in rows 8-12 rotor diameters apart in the windward direction, and 1.5-3 rotor diameters apart in the crosswind direction" (Grady et al., 2005:259). Because an array of fixed foundation turbines will necessarily be exposed to non-optimal wind directions on occasion, this rule of thumb is used to provide minimal losses. The Hexicon platforms are controlled to face the wind in an optimal way regardless of current wind direction, thus (potentially) reducing the need for turbine spacing as described above. In the H3-18MW platform the first and second row turbines are roughly 1.3 rotor diameters



(around 200 meters) apart in the windward direction, and the second row turbines are placed 1.3 rotor diameters apart in the crosswind direction. It is thought that with proper platform alignment, no wake induced losses should occur (Hexicon, 2013:3).

As the name suggests the H3-18MW platform consists of three nodes, supporting three turbines, rated at 6 MW each giving the entire platform an installed capacity of 18 MW. The platform's yaw axis (turret mooring) is positioned in the geometrical center of the structure. The platform itself is quite massive, 197 meters in length and a beam length (width) of 330 meters. The entire structure is estimated to weigh approximately 4,300 metric tons with the turbines installed carrying a full load draught of 15 meters (Hexicon H3-18MW, 2014:1). On each of the 10 meter diameter nodes sits a 6 MW offshore wind turbine.



Figure 2 showing an artist's rendering of the Hexicon H3-18MW platform at sea. Image from (Hexicon, 2014)

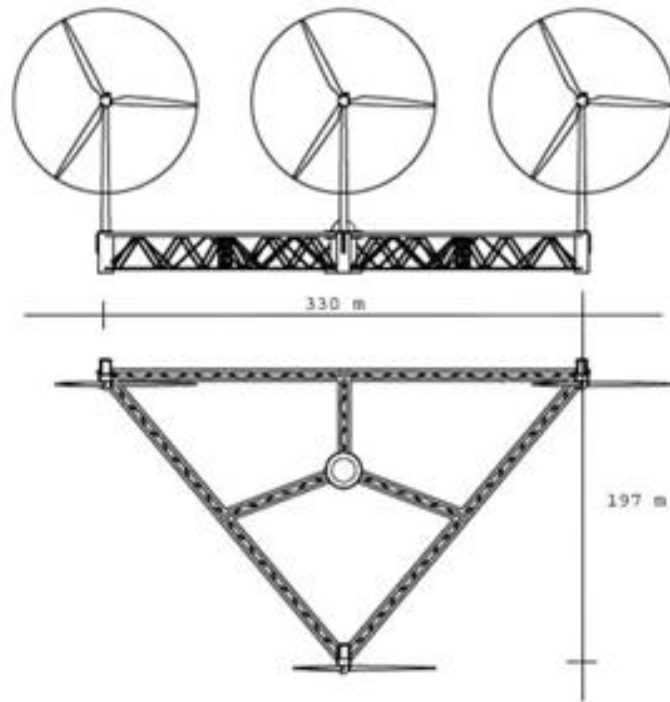


Figure 3 showing a schematic sketch of the H3-18MW platform with major dimensions. Note that the platform is assumed to lie stationary in the surge sway plane, with movement only possible in the yaw direction. The platform is anchored to the sea floor about the central turret in the middle. Image from Hexicon, 2014.

## 2.4 Dynamic positioning

Regardless of the specific techniques used to perform dynamic positioning (DP), DP is a process utilized by large ocean going vessels to calculate and hold (or move to) an exact position at sea despite the complex, even stochastic forces that continually act upon it (Chen et al., 2012:361). Dynamic positioning in present form finds its roots in the early 1960s gas and oil industry. As vessels (particularly oil rigs) became larger and the demand for accurate positioning on ever more troubled waters became acute, first mechanical, and later, computer based systems for automatic control were developed (Chen et al., 2012:361). In the interest of clarity it should be noted that much of the terminology used to describe the motion of ships has its roots in traditional nautical jargon. This report uses some terms that may be unfamiliar to the reader and an attempt to make clear the six degrees of freedom can be found in Figure 4. For use in this report the turbines are referred to as turbine(s) 1 to 3, where the leading turbine is denoted turbine 1, and so on moving clockwise about the platform.

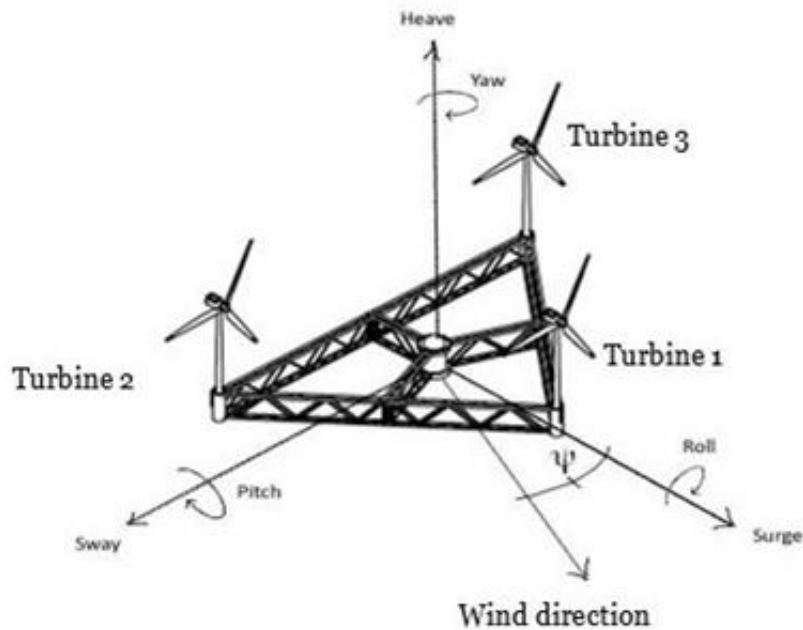


Figure 4 showing the H3-18MW platform, the 6 DOFs at sea, and individual turbine numbering as used throughout this report. For reference, the angle  $\psi$  is used to denote the (positive) platform misalignment relative the wind direction. Image modified with permission from Hexicon, 2014.

The first modern DP system was tested in March of 1961 onboard the *Cuss 1*. Originally the *Cuss 1* was designed and built in semi-secrecy as part of the American lead *project Mohole* (AMSOC, 1959:1) with the aim of drilling a 9,500 meter borehole through the earth's crust for geological exploration. Early in the planning stages of

*Project Mohole*, engineers in charge of sea keeping came to the realization that the drilling ship would need be confined to a radius of roughly 80 meters in the surge-sway plane (see Figure 4 for surge-sway definition). The solution to this problem would be found in a manually controlled, dynamic positioning system utilizing “... several large outboard-type motors...” to keep the *Cuss 1* within a ring of buoys. (AMSOC, 1959:1) *Mohole* was deemed a success, though soon greater demands on accuracy would push DP systems towards full automation (NAOS, 2011:1).

In late 1961, Shell introduced the Eureka, an oil rig outfitted with a fully automatic thruster driven dynamic positioning system which used taut wires (in lieu of the line of sight method used in the *Cuss 1*) for position feedback (Shatto, 2011:1). This was a major breakthrough in the offshore oil industry as Eureka was capable of drilling for oil at depths of 1000 meters, nearly 20 times the depth of her closest competitors at the time.

Since the 1960's, great improvements in dynamic positioning (DP) systems have been made. The principle behind the technique however is largely unchanged (Chakrabarti, 2005:1063). Reference positions for the vessel is set and continuous measurement of the ships positions is checked against these references. As deviations in the ships position arise, a new trajectory (or correction) is calculated using a real time regulator and the signals are sent to one or more thrust sources (traditionally a combination of thrusters and mooring lines (Chakrabarti, 2005:1063)(Balchen et al., 1980:135) which apply the correct thrust, in the proper direction, for the required amount of time.

In this sense a functioning DP system requires three elements; position measurement systems, a control system and a thrust source (Balchen et al., 1980:135). While DP control systems were originally outfitted with simple PID controllers for each rotational degree of freedom (surge, pitch, sway, roll, heave and yaw) modern methods have turned toward optimal control and Kalman filtering. This is largely due to the complex (and often interdependent) motions of ships which have shown to have a retarding effect on the integral action of PID controller, causing a delay in thruster response (Balchen et al., 1980:135). In more recent times, even Kalman filtering and optimal control methods have been widely replaced in nearly all DP systems with neural network control and fuzzy logic control techniques. These developments mostly due to increases in computing power and modeling accuracy (Chen et al., 2012:361). More than 50 years have passed since dynamically positioned vessels were first used, and it is currently estimated that over 2000 vessels actively use DP techniques to maintain proper sea keeping (Chakrabarti, 2005:361).

### **2.4.1 DP for the control of the Hexicon H3-18MW platform**

In terms of the Hexicon H3-18MW platform, it is suggested that a dynamic position system to control the heading of the platform relative the wind is designed. While preliminary designs of the platform have included thrusters (azimuth thrusters) a desire for simplicity has given rise to multiple possible solutions. In this paper, dynamic positioning using the wind turbines *themselves* as the source of thrust is investigated. Whether or not the turbine blades can be pitched in such a way the total thrust on the platform results in a turning moment, or torque, which can correct the platform's heading is investigated in this report. For detailed description of how this thrust arises, see the section (NREL turbine models)

The H3 platform is designed so that the axis of rotation is placed in the platform's geometrical center (see Figure 3). Alternative geometries/layouts could allow for the point of anchoring/rotation to be forward of the geometrical center which might allow for a more wind stable system, like a weathervane on a rooftop. This geometry however would be subject to the whims of ocean current, which often differs in direction and strength from the wind. The magnitude and direction of ocean currents are the result of many forces including tides, salinity and temperature gradients, the Coriolis effect, and sea bed contours and depths (Chakrabarti, 2005:729). Wind direction does have (to some extent) an impact on ocean currents though the extent of this influence is limited by depth and time. Wind systems do build ocean currents however due to the great inertial difference between the water and wind systems, a change of wave force direction (of significant magnitude) lags significantly behind the wind force direction. Even the direction of weaker surface currents can experience a lag of up to several hours following a change in wind direction (Chakrabarti, 2005:729).

Because the H3-18MW geometry places the rotational axis/mooring point, in line with the platforms geometrical center, the ocean current derived forces are always in balance, regardless of current direction and magnitude. Similarly the exposed platform (above the keel line) and the turbine towers also provide a zero net torque on the platform with respect to the rotational axis. The turbine blades however can be pitched; raising or reducing the torque on the platform.

Modern turbines are designed to follow the wind, and adapt the turbine yaw and pitch angle automatically, maximizing power production at each individual nacelle. Without a collective, coordinated control, turbines in a park have no interaction. Likewise, without such a coordinated control, simulations show the H3-18MW platform will rotate in and out of the wind in an uncontrolled manner (see section dealing with turbine modeling). The H3-18MW platform requires a dynamic positioning system.

Modern forms of dynamic positioning use a vast array of sensors, measuring devices and global positioning to relate the position of a vessel to its surroundings (Sørensen, 2011:1-6). Because the H3 platform is quasi stationary, (*movement is primarily restricted to the yaw direction*) the 6 DOF system is, in effect, reduced to a 1 DOF system and positioning the platform to face the wind becomes an altogether simpler problem. Because the platform is anchored to the sea bed, the geographical position is relatively unchanging, thus the need for global positioning systems is unnecessary. For this reason, only the wind angle (heading) relative the platform is needed for position referencing. To summarize, due to the large stability of the H3-18MW platform in pitch and roll, and the reduced need for translation in the surge-sway plane, this report investigates only 1-DOF (yaw) movements of the platform.

While conventional DP generally employs the use of thrusters for propulsion through the water (Sørensen, 2011:1-6) this adds complexity to the system. Thrusters require fuel and operational maintenance, which can be difficult to deliver to platforms situated far at sea. Furthermore, as the underpinning Hexicon concept of green, renewable energy production itself is somewhat tarnished by the use of fossil fuel driven thrusters, an alternative propulsion method is suggested. Without additional propulsion, the total thrust on each node, likewise the total turning moment, or torque exerted on the platform can be described as a function of relative wind speed, platform yaw misalignment and turbine blade pitch. At platform yaw misalignment, the torque produced from the turbines pushes the platform into non desirable positions where both power-production is lower and downwind turbulence is higher. This of course presumes the turbines are allowed to act as individuals producers. The aim of this project is to steer the platform into an optimal heading by controlling the individual turbine blade pitch. Pitching up the blades on one or more turbines, leads to a reduction in turbine thrust (see Figure 20). This phenomenon may be used to steer the platform. Because the turbines are limited at various wind speeds to a minimum blade pitch angle, the regulator used to control the system must be able to adapt to changing wind speeds. Moreover the complexity of the turbine platform system requires that the chosen regulator is capable of handling multi input, multi output (MIMO) systems. A model predictive controller (MPC) is capable of optimally handling MIMO systems with multiple input constraints (Vesely, 2010:5) and is therefore suggested as the automatic control system. MPC control has been widely researched by the DP community and is used in some vessels (Chen, et al. 2012:361).

### 3 Theory

In this section the theory used to explain the platform and turbine behavior is laid out. The theory portion of this work is used as a reference guide throughout this paper and covers themes ranging from control theory, systems identification, hydrodynamic theory and turbine theory. Furthermore the theory is written to stand apart from the rest of this work to be used as a reference for those readers who are interested.

#### 3.1 Hydrodynamic theory

A mathematical model of the platform is a necessary component in every modern DP system (Journée, et al., 2001:256). In order for an automatic controller to assess the amount of force or torque necessary to bring a vessel to a reference position a good understanding of a vessels hydrodynamic response to external forces is essential. In general it can be said that any sea going vessel has 6 degrees of freedom (DOFs); three translational directions (surge, sway and heave) and three rotational directions (pitch, roll and yaw), see Figure 4 for clarification. The motion of any vessel in this 6-DOF system can be described using a generalized equation of motion:

Equation 1

$$F_{ext}(t) = A\ddot{\xi} + D\dot{\xi} + S\xi$$

Where A is the mass matrix, D is the damping matrix and S is the restoring force (or stiffness) matrix. The external force  $F_{ext}(t)$  is the sum of all external forces (wave, wind etc.) acting on the vessel which give rise to a displacement in any direction of  $\xi$ . The mass matrix is the sum of the structural mass (M) and added mass ( $M_a$ ) matrices given as

Equation 2

$$A = M + M_a = \begin{bmatrix} m_{11} & \cdots & 0 \\ \vdots & \ddots & \vdots \\ 0 & \cdots & I_{nn} \end{bmatrix} + \begin{bmatrix} m_{11} & \cdots & m_{1n} \\ \vdots & \ddots & \vdots \\ m_{n1} & \cdots & m_{nn} \end{bmatrix} \quad M, M_a \in R^{6 \times 6}$$

The structural mass matrix M contains the physical mass of the vessel and the rotational moment of inertia. The added mass matrix contains the added mass constants for all DOFs. Added mass (a slight misnomer) is the additional *inertia* a structure/vessel acquires when accelerated in a fluid. This extra inertia is amassed as the fluid/ vessel system cannot occupy the same physical space at the same time, i.e. the fluid must be pushed out of the way (Journée, et al., 2001:256), (Tchet, 2005:2-

5). The damping matrix  $D$  contains coefficients pertaining to the effects of vessel/wave interaction, particularly radiation forces. The radiation force arises as incoming waves absorb some of the structures kinetic energy. The damping matrix  $D$  can be represented as

**Equation 3**

$$D = \begin{bmatrix} d_{11} & \cdots & d_{1n} \\ \vdots & \ddots & \vdots \\ d_{n1} & \cdots & d_{nn} \end{bmatrix} D \in R^{6 \times 6}$$

and the restoring matrix  $S$  is expressed as the sum of the hydrostatic ( $H$ ) and mooring line stiffness ( $L$ ) matrices, that is to say

**Equation 4**

$$S = H + L = \begin{bmatrix} c_{11} & \cdots & c_{1n} \\ \vdots & \ddots & \vdots \\ c_{n1} & \cdots & c_{nn} \end{bmatrix} + \begin{bmatrix} k_{11} & \cdots & k_{1n} \\ \vdots & \ddots & \vdots \\ k_{n1} & \cdots & k_{nn} \end{bmatrix} H, L \in R^{6 \times 6}$$

The hydrostatic forces acting on a vessel are the result of buoyancy related pressures and the elements of matrix  $H$  are largely geometrical properties (Techet, 2005:2-5). The mooring link stiffness matrix  $L$  is comprised of spring constants. The restoring force matrix  $S$  is comprised of constants relating to the hydrodynamic forces acting on the vessel which are proportional to the vessels velocity.

To fully understand the motion of a vessel a detailed analysis must be carried out and all constants must be determined. This type of analysis is usually carried out with help of specially designed FEM software and often physical models are built for verification (Techet, 2005:2-5), (Journée, et al., 2001:256). In lieu of complex, and time demanding computer simulations, the analysis of the forces acting on an ocean going vessel can be done using a number of semi-empirical models. Several different methods and theories exist i.e. diffraction theory, Froude-Krylov theory, and the Morison equations (Kurian, 2012:2), (Journée, et al., 2001:256). The choice of method depends largely on the type of structure, the dominating forces and the type of ocean environment the structure will be exposed to. Figure 5 illustrates one way to determine the dominating forces (and accompanying theories) given structure geometry and wave climate.



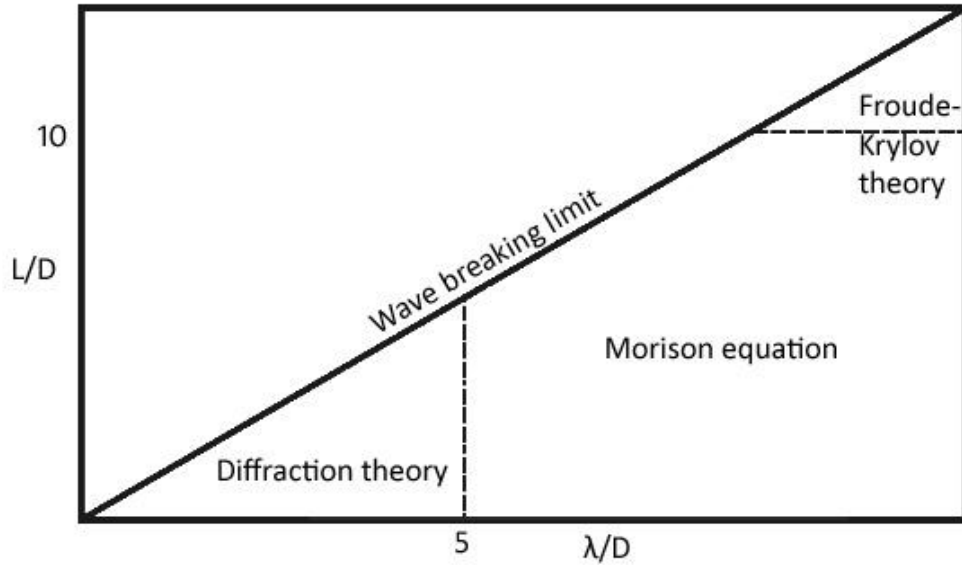


Figure 5 showing the regions in which different wave derived forces exist as a function of vessel geometry and wave climate. L and D denote the structural elements length and diameter respectively. The average wave length of the surrounding ocean environment is denoted  $\lambda$ . By identifying the relative location of the structural elements an appropriate theoretical description can be chosen.

As described earlier, the H3-18MW platform is comprised of many (slender) cylindrical elements. Moreover, water and waves are assumed to pass through the submerged structure without much interaction due to the relatively sparse construction (Lloyd's Register, 2008:3). For the majority of the structural elements the H3-18MW platform is comprised of, the Morison equation should give reasonable prediction for normal sea states (Finn, 2014:31)

The platform model created for this project is a hydrodynamic model based on the Morison equations for forces acting on a rigid body. The Morison equations assume that the inertial and drag forces are the dominating forces acting on the body. Moreover the body is assumed to be completely rigid, the liquid (sea water in this case) of a constant density and viscosity. With these forces in consideration, the geometry of the platform, the mass distribution contribute to the inertial force, and the wetted area of the submerged body contribute to the drag force as can be expressed as

Equation 5

$$r \times F = I \ddot{\xi}_{yaw} + \frac{1}{2} \rho C_d A \dot{\xi}_{yaw}^2$$

25

The Morison equation is shown above expressing angular acceleration and velocity in yaw. Here  $r$  is the distance between a point force and the axis of rotation,  $I$  is the platform moment of inertia,  $\rho$  is the density of sea water,  $C_d$  is the drag coefficient of the platform in water and  $A$  is the projected wetted surface area of the platform (at rest). This result closely resembles a 1 DOF version of the more general description of motion, where (in yaw) the mass matrix is simplified to the inertial moment of the platform about the heave axis, and the damping matrix is replaced by a drag based force. Because the platform is assumed to exert no force on the centrally placed mooring line in yaw, the restoring matrix here is the empty set.

### 3.2 Turbine theory

The three 6 MW turbines on the H3-18MW platform are described in this work using standard turbine equations based on Betz theory. For all calculations the wind can be considered laminar, with no vertical shear. The wind speeds experienced at each turbine are considered to be the free wind speed or a reduced wind speed as described by the Jensen wake model. Turbulence is ignored. Furthermore, each turbine is approximated as an actuator disc with an area equal to the swept area of the turbine rotor. Turbulence is ignored. The main turbine equations used in this work are shown in Equation 6 and Equation 7. Where the power produced is shown as

Equation 6

$$P = \frac{1}{2} \rho A |v| \cdot v^2 c_p$$

and the force exerted on the central axis of the turbine as

Equation 7

$$T = \frac{1}{2} \rho A v^2 c_t$$

In Equation 6 and Equation 7,  $\rho$  is the density of air,  $A$  is the turbine disc area,  $v$  is the wind speed relative the turbine and  $c_p$  and  $c_t$  are the power and thrust coefficients respectively. Betz law tells us that the maximum value of the power coefficient is  $16/27$  (about 0.593) and while the NREL 6-MW has a maximum value of 0.47, this value changes as a function of wind load and blade pitch. Betz law as first described in the early 20<sup>th</sup> century by German physicist Albert Betz, describes the total amount of kinetic energy that can be extracted from freely flowing wind by an actuator disc (read: wind turbine).

### 3.3 Wake theory

When modeling turbines that stand in a park, it is important to include the turbine wake interaction that occurs between the upwind and downwind turbines. Using wake model analysis (even simpler models) to aid in turbine siting, it is possible to increase total park performance and minimize structural loads due to turbine wake interference (Annoni et al., 2014:2517). This is because (in terms of energy capture) a turbine's wake is characterized by a reduced wind speed. The wake created behind a turbine is generally divided into two categories of wake types; near and far wake (see Figure 6). Up to a distance of 5 rotor diameters behind a leading turbine, 'near wake' behavior is exhibited, gradually fading into 'far wake' behavior. Near wake behavior is characterized and determined by the geometry of the upwind turbine, whereas 'far wake' patterns are determined more closely by atmospheric phenomena, pressure, temperature and wind speed (Annoni et al., 2014:2518). Because the turbines on the H3-18MW platform stand at 1.3 rotor diameters (roughly 200 meters) distance the trailing wake behind any leading turbine will be best characterized as 'near wake'.

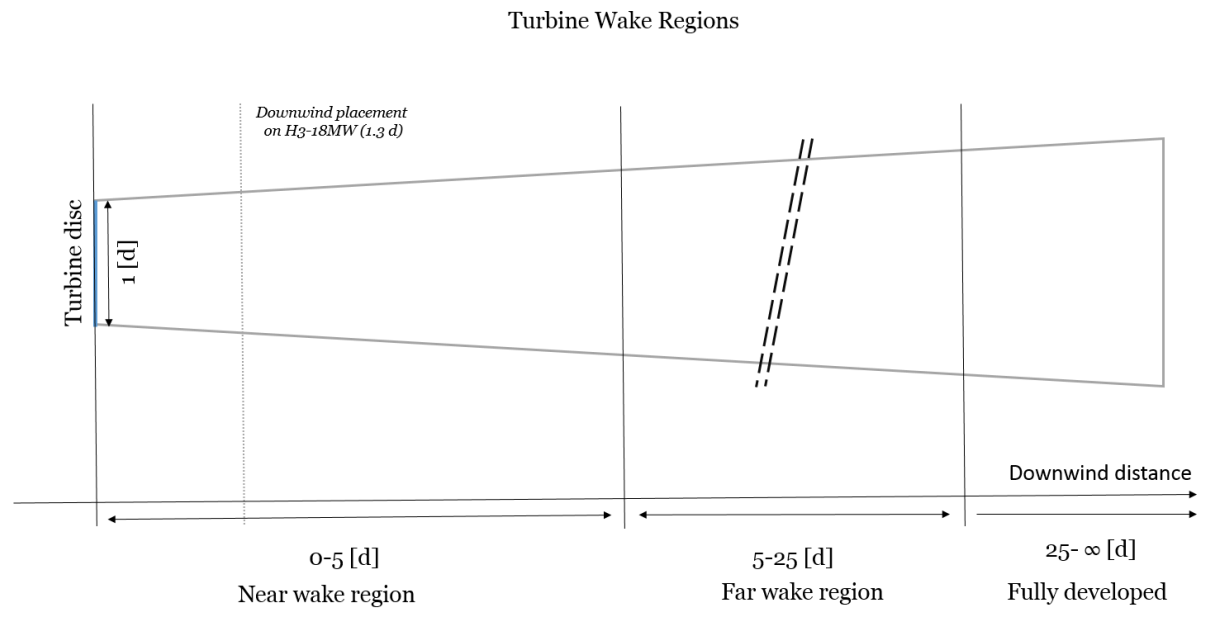


Figure 6 showing the wake regions developed downwind of a turbine. Note the break in scale in the far wake region. The shape of the wake shown as the grey trapezoid is based on the Jensen wake model described below. The diameter of the expanding wake is a function of the turbine disc diameter, the axial induction factor and the terrain shape factor  $k$ .

To model the wake field in and around the H3 platform the Jensen model is proposed as a first approximation model. The Jensen model (also known as the Park model)

simplifies the turbine to an actuator disk with a linearly expanding laminar (non-turbulent, non-rotating flow) wake (Annoni et al., 2014:2518), (Tong, 2012:1-13). This simplified model is expressed as a function of the upwind (wake creating) turbine's axial induction factor and the free (undisturbed) wind speed as can be seen below in Equation 8. The undisturbed wake speed is then

**Equation 8**

$$U_{wake} = U_{\infty} \left[ 1 - \alpha \left( \frac{D}{D + 2k_{wake}X} \right)^2 \right]$$

with the axial induction ( $\alpha$ ) factor expressed as

**Equation 9**

$$\alpha = (1 - \sqrt{1 - C_t})$$

Where  $U_{\infty}$  is the undisturbed wind speed,  $C_t$  is the thrust coefficient,  $D$  is the upwind turbine diameter,  $X$  is the distance downwind of the turbine, and  $k_{wake}$  is the wake decay constant which for offshore climates is suggested to be around 0.05 [-] (Barthelmie et al., 2005:476). In this way an effective lowering of the thrust coefficient (blades pitching up) allows for less wind energy to be extracted by the upwind turbine, while allowing for a higher average wind speed in the wake and the downwind turbine. The Jensen model is usually considered a 'lo-fi' model in that many mathematical simplifications are made to explain wake behavior. Despite this, the Jensen model is widely used within the industry to give a first approximation of wake induced velocity deficit downwind, as this factor is critical to turbine placement (Barthelmie et al., 2005:476), (Sørensen et al., 2006:1-6). Other, more advanced methods of wake analysis exist i.e. Larsen, Frandsen, Ishihara and Ainslie wake models, to name a few (Renkema, 2007:8). Several of these models build on the Jensen model but are more detailed, including parameters for hub height and turbulence intensity etc, giving more nuanced approximations of downwind climate (Tong et al., 2012:1-13) (Renkema, 2007:8). The Jensen model has however been shown to provide reasonable approximations of wake induced velocity deficit at distances  $>3$  turbine diameters (Barthelmie et al., 2005:476). The accuracy of the Jensen wake model at downwind distances less than 3 turbine diameters is difficult to measure accurately as this region is comparatively turbulent compared to the far wake and fully developed regions. For reasons of simplicity however, the Jensen wake model is used in this report as a first approximation of downwind velocity deficit.

### 3.4 System identification

To use MPC control, the solvers available in MATLAB and SIMULINK are dependent on linear models/representations of the system. In order to create a linear representation of the H3-18MW platform, turbines etc., first a systems model comprised of the hydrodynamic, the aerodynamic and electromechanical components is created. From this system model, system identification is used to approximate a state space representation which can be used with the MPC controller. While much of the system can be expressed mathematically through known physical relationships, other nonlinear elements make the creation of a white box model difficult. White box modeling is essentially a fully developed (true) model of the system, comprised entirely of differential equations derived from physical laws. Because of the nonlinearity of the aerodynamic properties of (for example) the turbine blades, white-box modeling becomes increasingly difficult. Therefore for the purposes of this report, a simulator which takes aerodynamic relationships from lookup tables and combines this information with mathematical descriptions to produce synthetic output data. From this data, a simplified linear model is approximated and used in the control schedule. This type of modeling is known as black box modeling, as the system is identified solely from inputs and output signals as described below. For more information concerning possible techniques for system modeling see the section entitled (9 Future works).

Impulse/frequency response analysis is used to assess the dynamic response of a system over a wide range of frequencies.

Given a linear system with an input  $u(t)$  as a sinusoidal signal with amplitude  $u_0$  and frequency  $\omega$  as,

**Equation 10**

$$u(t) = u_0 \cos(\omega t)$$

The system  $G(s) = G(i\omega)$  will produce the output signal  $y(t)$  as seen below,

**Equation 11**

$$y(t) = y_0 \cos(\omega t + \varphi)$$

Thus, the frequency response function of the system  $G(i\omega)$  can be described as a transfer function between the input  $u(t)$  and the subsequent output  $y(t)$  as is seen here: (Glad & Ljung p. 200-60 1994)

**Equation 12**

$$y_0 = |G(i\omega)|u_0$$

**Equation 13**

$$\varphi = \arg G(i\omega)$$

To attain the total system frequency response (the response over a greater frequency spectrum), input signals (wind speed, platform misalignment, and the three blade pitch angles) are supplied as pseudo random binary sequences (PRBS). A PRBS is an input signal  $u(t)$  that varies in a binary fashion over time. The output signal  $y(t)$  contains information about the systems behavior over the frequency spectrum of the chosen input PRBS. In nonlinear systems, the amplitude of the input signal will affect the behavior of the system, thus it is important to run many tests with varying input signal amplitudes to see how the system behaves overall operating conditions.

It is likely that due to the complexity of the studied systems, and importantly, as a result of the theory presented in the sections dealing with hydrodynamic, and aerodynamic properties that the H3-18MW platform system is non-linear in nature. A nonlinear system is exemplified itself as a system which does not follow the superposition principles of linear systems, described above in Equation 10-Equation 13. That is to say that an identified linear system once expressed for one input frequency and amplitude, will not necessarily produce the same/expected behavior at different input frequencies and amplitudes. This distinction can be expressed as the result of feedback noise in the closed loop system, where noise is here essentially an expression for the nonlinear aspects of the system. In terms of identifying linear expressions of inherently nonlinear systems, one may employ what is known as best linear approximation (BLA). BLA of a nonlinear system is an approximation of that system which "... minimizes the difference between the actual output of the system and the modeled output in a least square sense". (Wong et. Al., 2013: 519) As is likely with this method, any attempt at linear approximation of this system (even a BLA) will result in a loss of information, in terms of system dynamics. It is therefore important that several identification methods, and model orders be tested to ensure the best possible linear approximation is found, despite inherent inaccuracies in this generalized approach.

### 3.5 Model predictive control

Model predictive control (MPC) is a digital, embedded (real-time) control method developed in the 1970's, originally for use in the chemical and oil industries. (Boyd, lectures 2010) The basic problem MPC tries to solve is a common control problem that can be expressed as follows:

A solution shown in Equation 14 is found as

Equation 14

$$\min (J) = \sum_{\tau=t}^{t+T} C[x(\tau), u(\tau)]$$

Where  $x$  contains the states of the system and  $u$  comprises the inputs. Both states and inputs are subject to the constraints shown in Equation 15. The inputs bound as

Equation 15

$$u(\tau) \in \mathbb{U} \text{ and } x(\tau) \in \mathbb{X} \quad \forall \tau = t, 1, \dots \infty.$$

In this case the inputs  $u$  are restricted to bound set  $\mathbb{U}$  and  $x$  to a similar bound set  $\mathbb{X}$ . By minimizing  $J$ , the cost function is reduced. The cost function in control theory refers to a mathematical minimization problem, in which a trade-off between the 'cost' of executing an input signal and the benefit/reward of coming close to a reference signal or state is made. (Glad & Ljung, 2005)

This type of problem is common to many types of optimal control problems; however model predictive control has specific method for synthesizing inputs. The MPC controller appends additional criteria for minimizing  $J$ , by imposing a finite time horizon (also known as the control horizon)  $T$  as follows in Equation 16:

Equation 16

$$u(\tau) \in \mathbb{U}, x(\tau) \in \mathbb{X}, \forall \tau = t, \dots, t + T$$

Such that the system states are driven towards a minimum by time  $T$  as

Equation 17

$$x(\tau + 1) = Ax(\tau) + Bu(\tau), \forall \tau = t, \dots, t + T - 1$$

so that at time  $T$

Equation 18

$$x(t + T) \cong 0.$$



This effectively reduces the infinite dimensional subspace  $t \in \mathbb{R}^\infty$  to a finite dimensional subspace  $T \in \mathbb{R}^n$ , and drives the states in  $x$  to near zero (or some reference value) by time  $T$ . This is not an optimal solution in mathematical terms because the infinite subspace has been reduced, and information is lost. However, for many systems, the cost function  $J$  converges quickly in time and additional dimensions of  $t$  above some value  $T$ , are not necessarily useful from a control standpoint (Boyd, Lectures 2010). For significantly long control horizons  $T$ , the result is near an optimal solution.

Below, in Figure 7, a graphical representation of the MPC process illustrates how the controller works in practice.

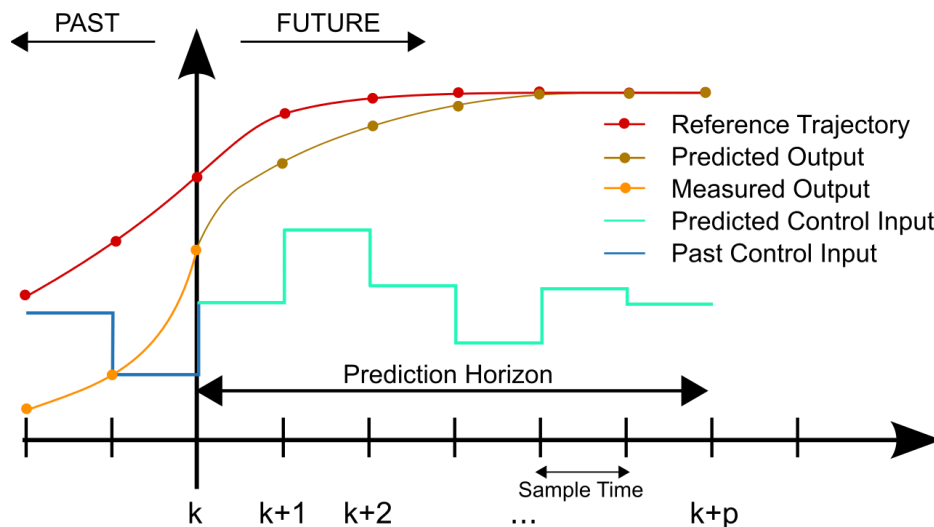


Figure 7 showing the operating principal behind MPC control. The current states are measured and given output limitations, the controller predicts optimal strategies to reach the reference trajectory within the prediction horizon. Image from Wikipedia (MPC control, 2014)

To predict the string of inputs the controller acts as follows: at time  $t$ , the current states of the variables are measured (observed, denoted  $\hat{x}$ ) using a Kalman observer, and these measured states are used as a starting point. A planning exercise is carried out which propagates the states forward within the event horizon time  $T$ , insisting that at time  $T$  the states ( $\hat{x}$ ) reach zero. After the inputs ( $\hat{u}$ ) are calculated for the entire event horizon, the states and inputs are collected as

Equation 19

$$\hat{x}(t + 1), \dots, \hat{x}(t + T) \ \& \ \hat{u}(t), \dots, \hat{u}(t + T - 1)$$

At this point the regulator implements control task  $\hat{u}(t)$  and *the remaining control actions are discarded*. Only the first input signal is retained after each iteration, in practice the solution comes very close to the optimal solution in an infinite control horizon- despite constraints on  $u$  and  $x$ . This of course presupposes limited system stochasticity and measurement noise (Boyd, Lectures 2010).

The controller then returns to the beginning, measures the states and the process is repeated for the next time step (Glad & Ljung, 2003), (Boyd, 2010). While this process is not optimal in the mathematical sense, very good results have been obtained historically, especially for slower processes (Boyd, Lectures 2010). Because the future inputs  $u(t)$  are computed with no regard to the input/output restrictions, the actual system input signals can differ from the solution which originally minimized the cost function.

Furthermore, in this work attempts have been made at designing a multi-objective MPC controller. Multi-objective control can be defined as a tunable MPC controller that optimizes output signals such that two or more objectives are met simultaneously. The controller used in this thesis aims to maximize power production while minimizing platform misalignment relative the moving wind reference signal.

## 4 Method

The method section of this work lays out the general process used to create a platform simulator, approximate a linear system based on simulated results (synthetic data), and lastly, control of the approximated linear system.

### 4.1 Modeling in general

The models of the entire system can be divided into three types; a hydrodynamic model (of the platform interaction with the ocean environment) an aerodynamic model (turbine wake model and turbine blade efficiencies) and an electromechanical model describing the turbines power and thrust production. MATLAB is used extensively in this work, applying the various theoretical methods to the H3-18MW platform. For visualizations of the individual models, see the section entitled results.

To create a complete model of the system, each of these models are combined in a single MATLAB script represented visually in Figure 8.

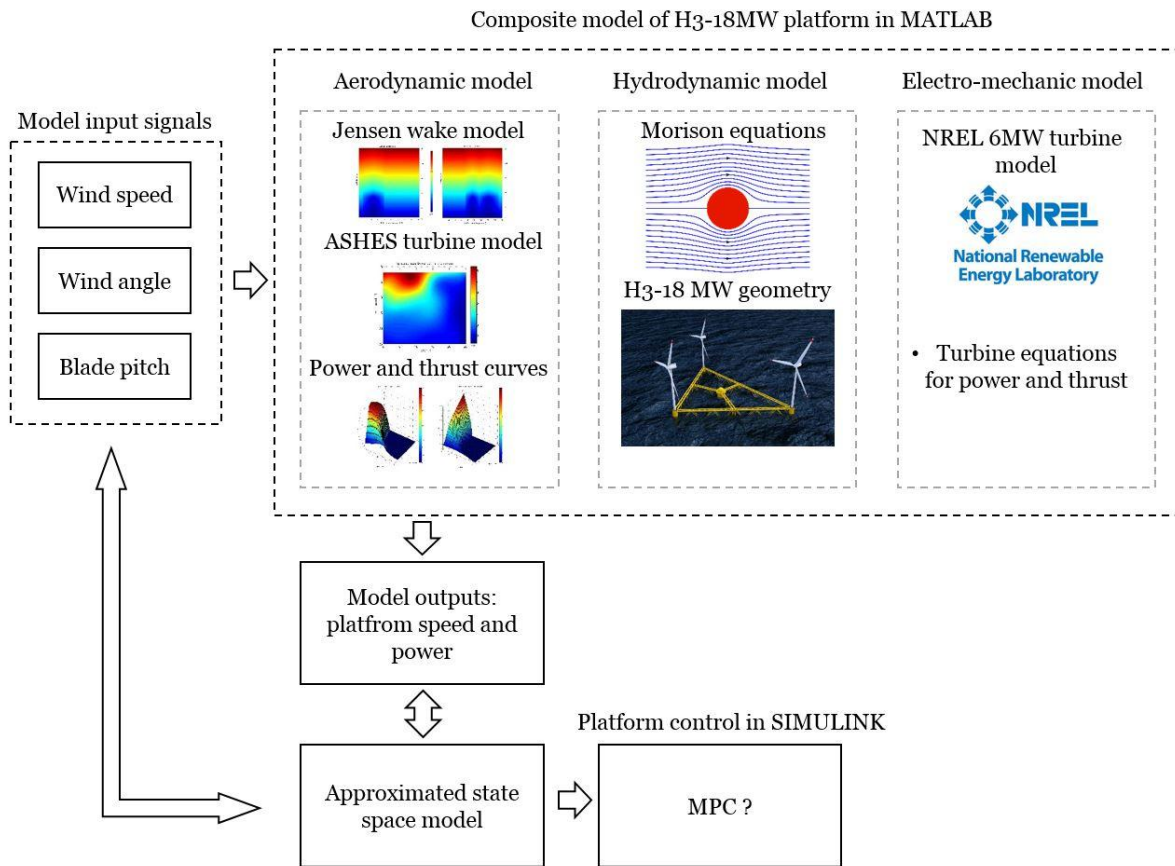


Figure 8 showing the composite H3-18MW platform, system inputs and outputs. The MATLAB model is used to generate synthetic data for systems identification and later, control.

The Aerodynamic model is comprised of the Jensen wake model (Figure 13, and Figure 14), the sub-optimal blade pitch TSR's calculated in ASHES (Figure 19), and the Scandinavian wind generated  $C_p$  and  $C_t$  curves (Figure 22 and Figure 23). These

combine with lower limit blade pitch settings (Figure 18), electromechanical models (Turbine equations) and the Morison hydrodynamics model (Figure 10) in a single MATLAB script to two system outputs, Power and platform yaw speed (angular velocity).

## 4.2 Linear model approximation

The platform, wake and turbine models are combined in several MATLAB programs that work together to describe the platform rotational velocity and power output as a function of time, wind speed, platform angle and turbine blade pitch values. As the model predictive controller requires that the system be described in state space form (see section on MPC) the system is approximated using a combination of impulse (frequency analysis) and MATLAB's System Identification Toolbox (SIT). The frequency analysis is based on the theory covered in the section entitled Theory, 1.2 system identification, using Equation 10 to Equation 13. The signals used as inputs to the platform simulator are PRBS signals with primarily low frequency content (10e-3 to 10e-1 Hz). Earlier attempts to categorize the system showed system excitation in this region. PRBS signals are commonly used in system identification as a simple way to test the system's response to a wide range of frequencies.

Before attempts at system identification can be made, a spectral analysis of the various input/output subsystems is carried out. Because the platform/turbine system is described using a combination of linear and nonlinear relationships, it is unclear if the system *can* be approximated with a single, linear, time invariant model. Several simulations are run at different operational points and data is collected. 6 separate tests are run with varying PRBS signal amplitude and spectral models are compared to identify differences in static gain, frequency response, possible system order, etc. These scenarios are predetermined and can be found in Table 5.

Table 5 showing the various PRBS signal values for each input respectively. These inputs are varied, and illustrate in the spectral analysis, the non-linearities of the system as a whole. Note the blade pitch input (lower bound) is determined by the wind speed in the event 0 degrees (blade pitch) is below rated pitch.

Test name	Wind speed [m/s]	Wind angle [°]	Pitch (collective) [°]
Test 1	0-16	0-5	0-25
Test 2	0-16	0-5	0-25
Test 3	0-10	0-10	0-25
Test 4	0-22	0-0.01	0-25
Test 5	0-12	0-5	0-25
Test 6	0-10	0-15	0-25

Spectral approximations of each data set show the nonlinear behavior of the system. The results of the spectral analysis can be seen in the results section in Figure 27 and Figure 28.

### 4.3 Control with SIMULINK model

Approximated H3-18 MW state space models for angular velocity and power production are implemented in Simulink and connected together as seen in Figure 9. Blade pitch and power limitations are created as functions of wind speed and added to the model. Lastly the MPC regulator is designed and scenarios and platform models are loaded into the simulating environment. Note in Figure 9 that the reference signal for the platform yaw angle is set to a constant zero, and the first measured output signal is the difference between the wind angle and the platform angle. This is equivalent to a coordinate system which rotates with the wind, the platform angle error is then the expression of the angular distance from the platforms optimal orientation to the oncoming wind. Furthermore the wind speed and angle signals are assumed to be a calculated average wind speed and angle observed by the park as a whole. This assumes that the wind system is larger (in size) than the platform system, which is deemed to be a reasonable assumption for these simple scenarios.

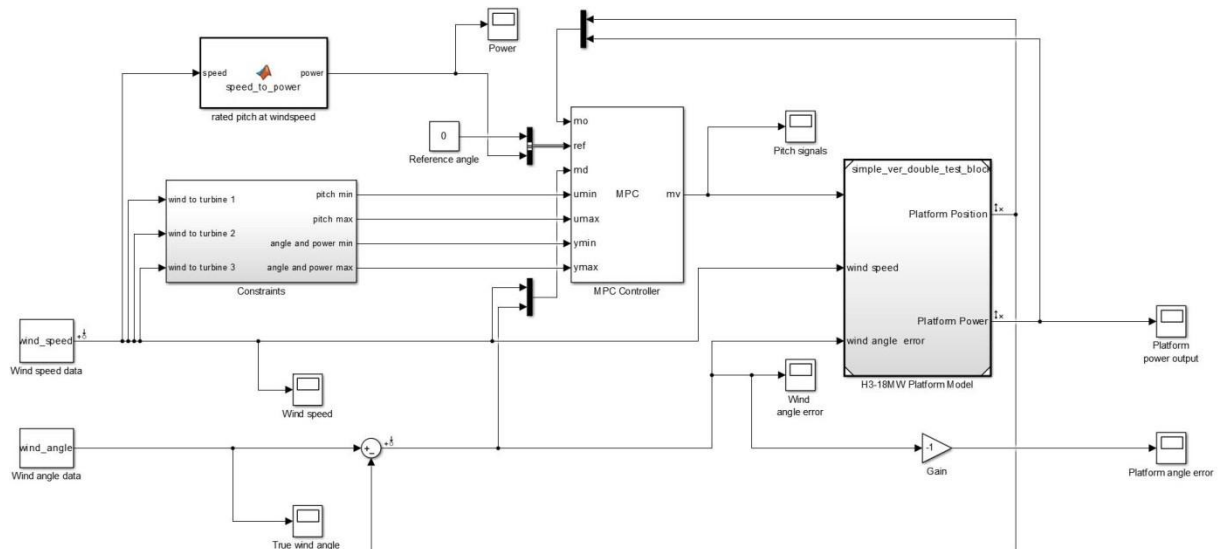


Figure 9 showing the SIMULINK model of the H3-18MW platform as controlled with a multi-objective MPC controller.

Early attempts using the SIMULINK MPC controller showed erratic, unintuitive controller behavior which, in a word is, unexplainable. Due to the unresolved technical issues with SIMULINK, and time constraints on this project, the MPC controller was never found to function properly. Outreach within the online MATLAB (Mathworks) community confirmed the existence of underlying software problems which have yet to be resolved in the available beta version of the MCP toolbox. Final results will instead employ a simpler logical controller which allocated blade pitch in such a way that the total torque output from the turbines on the platform is in the

direction of the wind angle error. Though this control method is perhaps ill suited to the regulation problem at hand, it may showcase the controllability of the platform in general. To check the viability of the controller and the platform speed and power production during yaw maneuvers, several tests are devised. These tests have been predetermined to showcase different aspects of controllability and platform dynamics as seen below in Table 6

For testing the system under regulation several scenarios are devised to explore the strengths and limitations of the system as a whole. The specifics of the scenarios are shown in Table 6 as well as in Figure 32, Figure 34, Figure 36, and Figure 38. A simulation time of 300 (5 minutes) seconds is used in each scenario.

**Table 6 showing the scenarios used in controller testing.**

<b>Scenario</b>	<b>Wind speed profile</b>	<b>Wind angle profile</b>	<b>Comments/purpose of simulation</b>
<b>1</b>	Constant 15 m/s	Step from 0 to +15 degrees at time $t = 0$ .	Step response, establish base scenario.
<b>2</b>	Linear increase from 5 to 17 m/s	Step to +5 degrees at time $t = 0$ .	Step response, test with change in wind speed.
<b>3</b>	Constant 15 m/s	Linear increase from 0 to +10 degrees	Test platform dynamics with changing angle input.
<b>4</b>	Linear decrease from 25 to 20 m/s	Linear increase from 0 to +10 degrees.	Combination for comparison with above scenarios



## 5 Results

The results of this work are separated here into three sections, the first dealing with modelling of the platform, and the individual sub-models that comprise the main aggregated MATLAB simulator. Following this, the results of the frequency analysis and system identification in which the state space representation of the platform is determined. Lastly the control of the platform and the results from several trials are shown.

### 5.1 Platform models

The first major result of this thesis is focused on the MATLAB model of the H3-18MW platform, comprised of hydrodynamic, aerodynamics and electro-mechanic representations of the platform and turbines. In this section the sub-models which comprise the main model are shown, categorized after type.

#### 5.1.1 Hydrodynamic model

To visualize the platform dynamics the moment of inertia was calculated and the Morison equation (from theory Equation 5) was built into a simple program. A force is applied to the three corners of the platform in attempt to yaw 35 degrees. The results of this simulation are shown below in Figure 10.

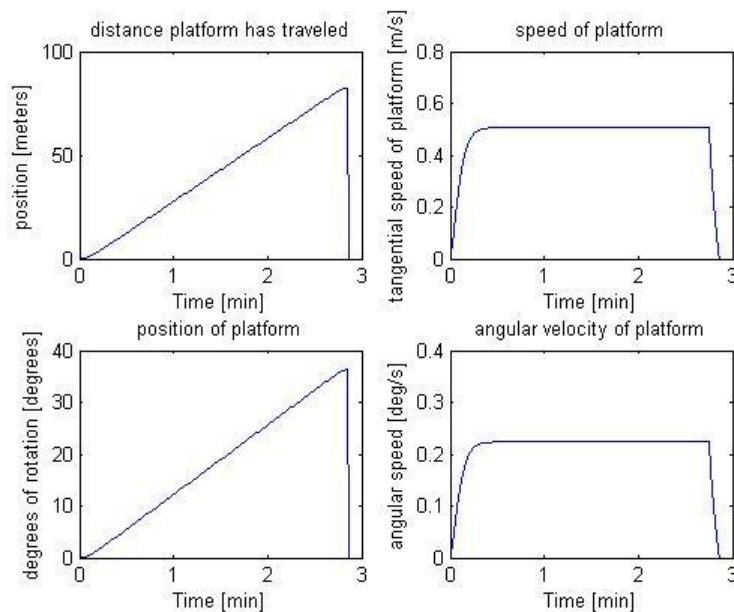


Figure 10 showing the platform behavior due to an induced torque. Clockwise from the upper left, the figure shows the instantaneous distance the prow of the platform has traveled (linearly during rotation), the instantaneous linear velocity of the platform prow, the instantaneous angular velocity of the platform during rotation, and the lastly the instantaneous angular position of the platform. Note the initial acceleration of the platform is followed by a period of constant velocity and concluded with a 'breaking' period where the drag of the water on the platform slows it to a complete stop around 3 minutes.

### 5.1.2 Aerodynamic models; wake and blade behavior

Different angles of platform misalignment will affect the downwind turbines due to wake interference. To illustrate this, the following plots (Figure 11 and Figure 12) show the wake area of the upwind turbine wake projected on the downwind turbine disc for various angles of platform misalignment. Only 180 degrees of platform misalignment are shown due to symmetry. Note: though the wake of an upwind turbine expands to an area larger than that of the downwind turbine disc, the total wake area the downwind turbine can be exposed to is the area of the downwind turbine itself.

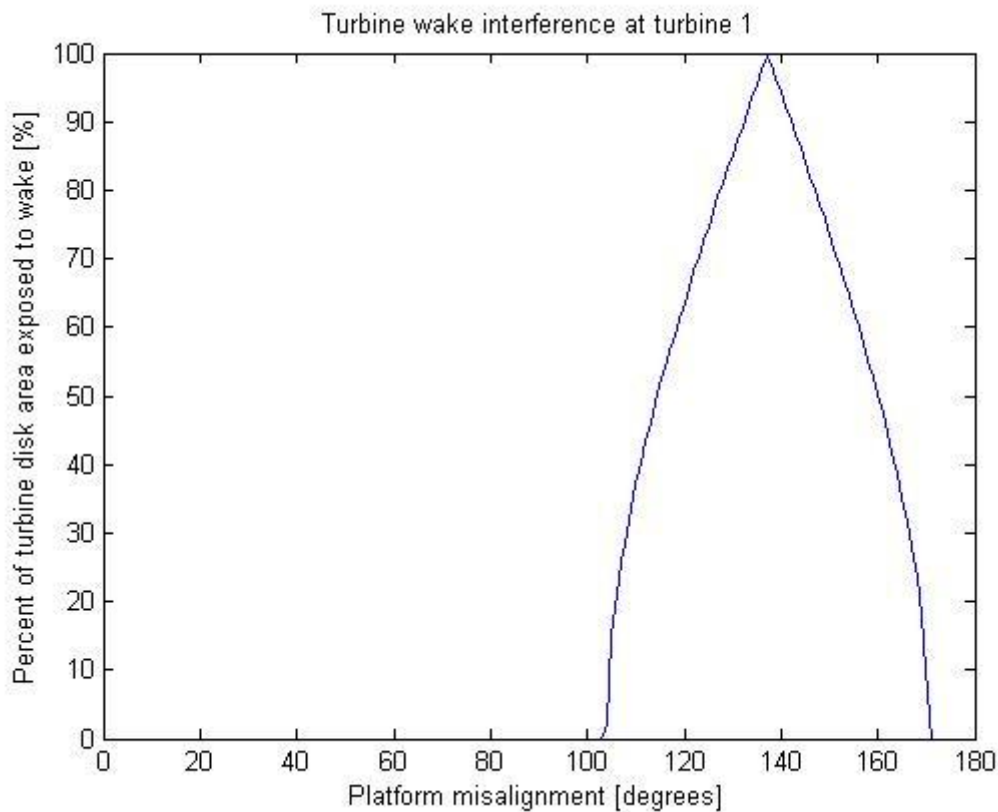


Figure 11 showing area of wake interference on turbine 1 (leading surge turbine) as a function of platform yaw misalignment as predicted by the Jensen wake model. As the wind angle increases to 100 degrees error, turbine 1 becomes completely shadowed by the wake of turbine 2.

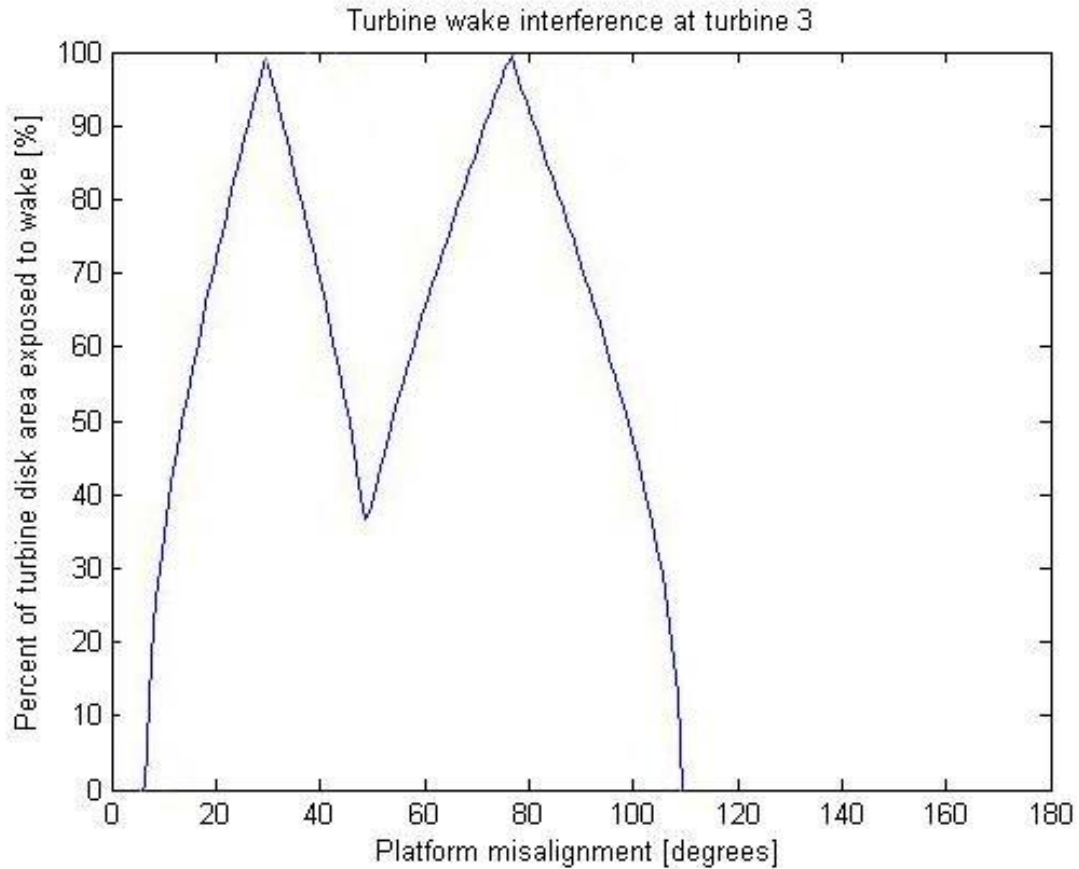
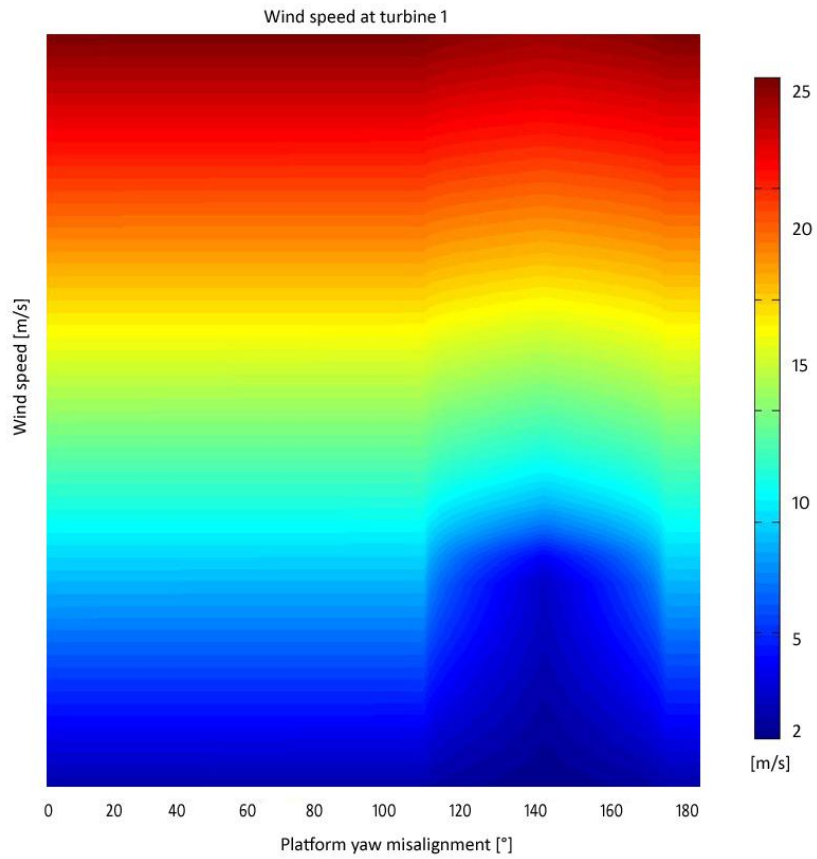


Figure 12 showing the area (percentage of the swept turbine area) of wake interference on turbine 3 (trailing sway turbine) as a function of platform misalignment as predicted by the Jensen wake model. Turbine-wake interaction becomes first apparent around  $\pm 3.5$  degrees.

The average wind velocity at the downwind turbines as described by the Jensen model is shown below in Figure 13 and Figure 14 as a function of platform misalignment and the free wind speed. Note that this diagram is shown for rated pitch angles and only expresses the maximum wind speed deficit at down wind turbines. While the wind speed variations due to wake interaction may seem small- the effective power delivered by a turbine is proportional to the cube of the wind speed, likewise; the torque from a turbine on the platform is proportional to the square of the wind speed.



**Figure 13** showing the average wind speed at turbine 1 (leading surge turbine) as predicted by the Jensen wake model. Note the greatest wind speed deficiency is near 140 degrees, as turbine 2 completely shadows turbine 1 with its wake. The deficiency is moreover greatest around 10 m/s as the thrust coefficient peaks at this wind speed.

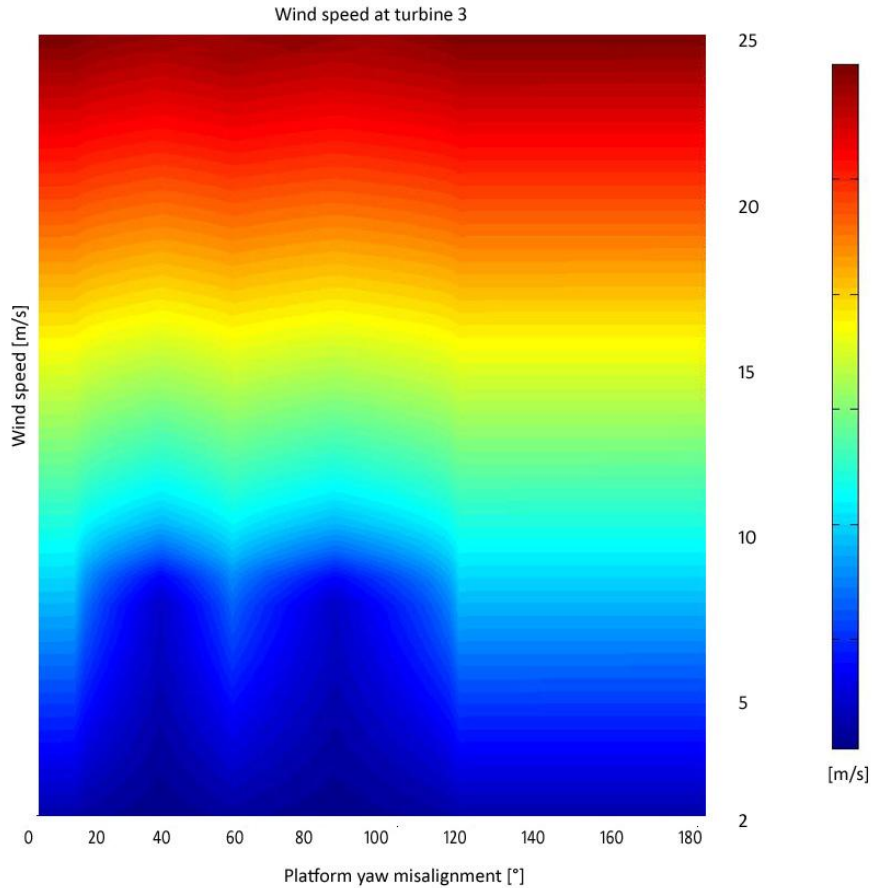


Figure 14 showing the average wind speed at turbine 3 (second row, lagging sway turbine) as predicted by the Jensen wake model. Note the difference in wake diameter. This is due to platform geometry as turbine 1 is roughly 250 meters from turbine 3, whereas turbine 2 is 330 meters upwind. See theory 1.3 wake theory for a more thorough explanation.

The wake model for the H3 platform is incorporated into the turbine models and a base line scenario is established for rated blade pitch at all wind speeds and platform yaw misalignment angles as seen below in Figure 15-**Error! Reference source not found.** This surface model is used later to compute the torque produced by each turbine given specific pitch signals.

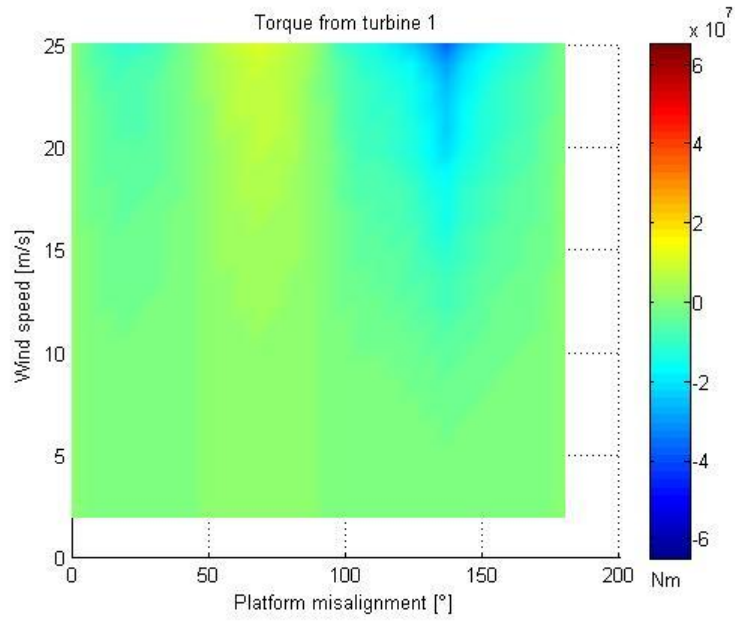


Figure 15 showing the torque output from turbine 1 on the H3-18MW platform for all wind speeds and platform misalignments. The turbine operates at rated blade pitch angles.

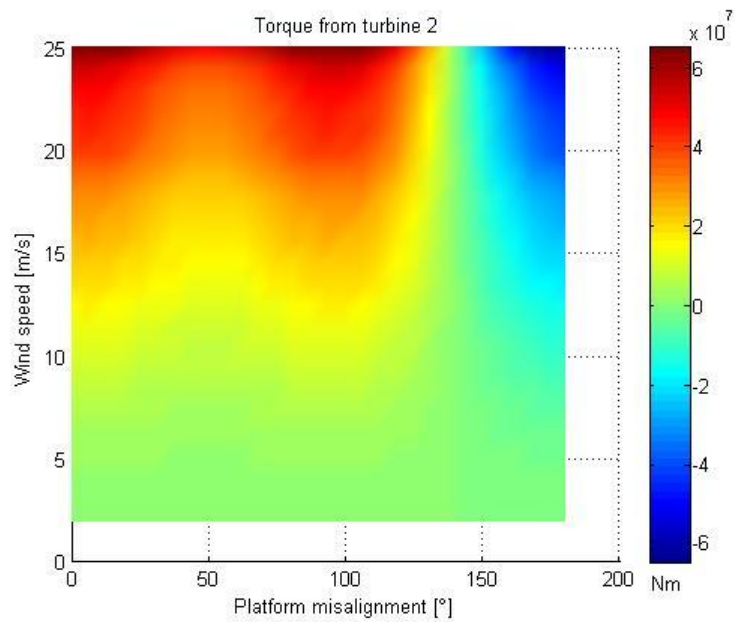


Figure 16 showing the torque output from turbine 2 on the H3-18MW platform for all wind speeds and platform misalignments. The turbine operates at rated blade pitch angles.

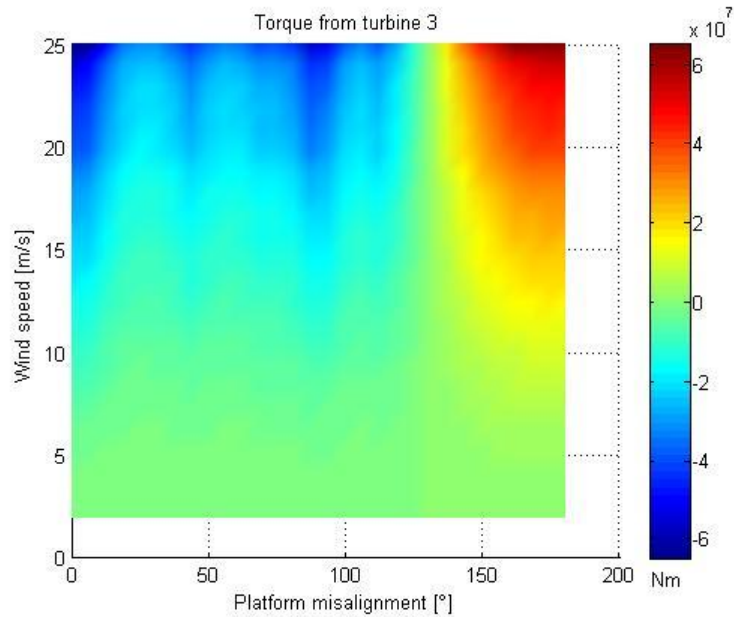


Figure 17 showing the torque output from turbine 3 on the H3-18MW platform for all wind speeds and platform misalignments. The turbine operates at rated blade pitch angles.

Figure 15 to show the torque produced at each turbine given nominal blade pitch values for the entire range of platform yaw misalignment angles and wind speeds. Under analysis one can see how the platform geometry affects the generated thrust. Likewise the effect of the Jensen wake model's downwind wind speed predictions can be seen to affect the torque output for various misalignment angles.

To this point the turbine models have been described from data prepared in 2014 by Scandinavian Wind AB and show the platform's turbines acting at *rated* blade pitch angles at given wind speeds. When analyzing Figure 15, Figure 16, and Figure 17, one can see the role played by turbine placement (platform geometry) with respect to the torque exerted on the platform. Near 0 degrees heading, the platform is initially quite stable, however, given large enough deviations in wind direction, the platform is simply at the mercy of the wind. Unregulated, the platform can fasten between peaks of positive torque (for example around 40 degrees at wind speeds above 15 m/s). Moreover, one can see at lower wind speeds (below 10 m/s) the unregulated platform experiences nearly zero net torque from the turbines. This seems to imply that the platform yaw will be relatively unaffected at low wind speeds (regardless of wind direction). Due to symmetry, these phenomena will also occur for negative deviations in platform/wind alignment.

In order to regulate and control the torque on the platform, one must force the turbines to produce a thrust (and therefore a turning moment) on the platform which corrects the heading. This can be accomplished in two ways; a turbine blade pitch can be reduced, thus increasing the turbine thrust on the platform, or inversely, the

turbine blade pitch can be increased, reducing the thrust. Due to electrical limitations in the turbine drive chain, the turbines may never be run at blade pitch angles which collect more power from the wind than the generator is rated for, that is to say, the nominal blade pitch angles are the lower bound (see Figure 18 below). An increase in blade pitch angle is always a technically possible, as the effective power collected in the generator is simply reduced. In order to protect the machinery then, one or more of the turbines must be run at sub/optimal pitch angles. By increasing the pitch angle in a given wind, the tip speed ratio will be reduced and less power and thrust will be delivered from the turbines. The resulting reduction in torque can then be utilized to turn the platform into the oncoming wind. It is this technique the DP system will utilize to control the yaw of the H3-18MW platform.

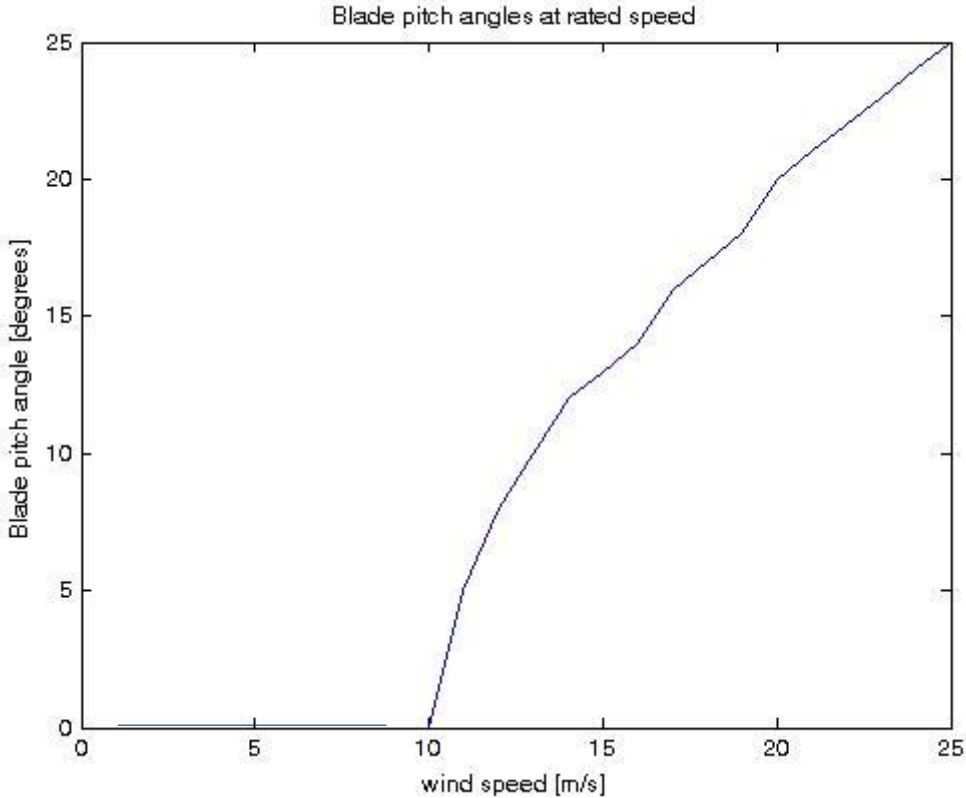


Figure 18 showing rated blade pitch for all wind speeds between 2 and 25 m/s (cut in and cut out speeds)

Data for turbine performance does not generally exist for sub-optimal operation points and must therefore be estimated. The blades of the turbine are optimized such that the turbine will obtain a maximum global power coefficient and corresponding optimal tip speed ratios for given wind speeds. To do so, blade parameters including section length, twist and chord length are chosen according to a design law which ensures a global maximum aerodynamic efficiency (Dosaev et al., 2014:402-9). The



terms *global power coefficient* and *global aerodynamic efficiency* simply refer to the performance of the blade as a whole.

Using the finite element method (FEM) analysis program ASHES, developed at Norges teknisk-naturvitenskapelige universitet (Norwegian university of science and technology) the NREL 5MW turbine was tested for a variety of wind speeds and pitch angles without the default PID controller activated. Ashes, is a time domain, FEM program designed for simulation and development of offshore wind turbines (Thomassen, et al., 2012:374). Because the blade geometry is simply scaled with a ratio of 1:1, and TSR and rotor speed are similar for similar wind speeds the results of this analysis are deemed practical for use in the NREL 6MW turbine model as well. Because the turbine will perform sub-optimally at sub-optimal blade pitch settings in a given wind, care was taken to find rotor speeds (and complimentary TSRs) which produced the highest power rating at each sub-optimal blade pitch. In this way the turbine is allowed to produce energy as optimally as possible despite the sub-optimal blade pitch settings. The following table (table 3) shows the data collected from this analysis. Below Table 7, Figure 19 shows an extrapolation of this data set presented in 3-dimensions.

Table 7 showing the TSRs at sub-optimal blade pitch values as calculated using ASHES.

<b>Blade Pitch</b>	<b>0</b>	<b>5</b>	<b>10</b>	<b>15</b>	<b>20</b>	<b>25</b>
<b>Wind speed</b>						
<b>2</b>	8	6.5	4.2	3.3	2.6	1.95
<b>5</b>	8	7.2	5.8	3.3	2.6	2.1
<b>10</b>	8	7.5	4.6	3.3	2.6	2.1
<b>15</b>	-	-	-	5.5	2.5	2.0
<b>20</b>	-	-	-	-	4.2	2.1
<b>25</b>	-	-	-	-	-	3.3

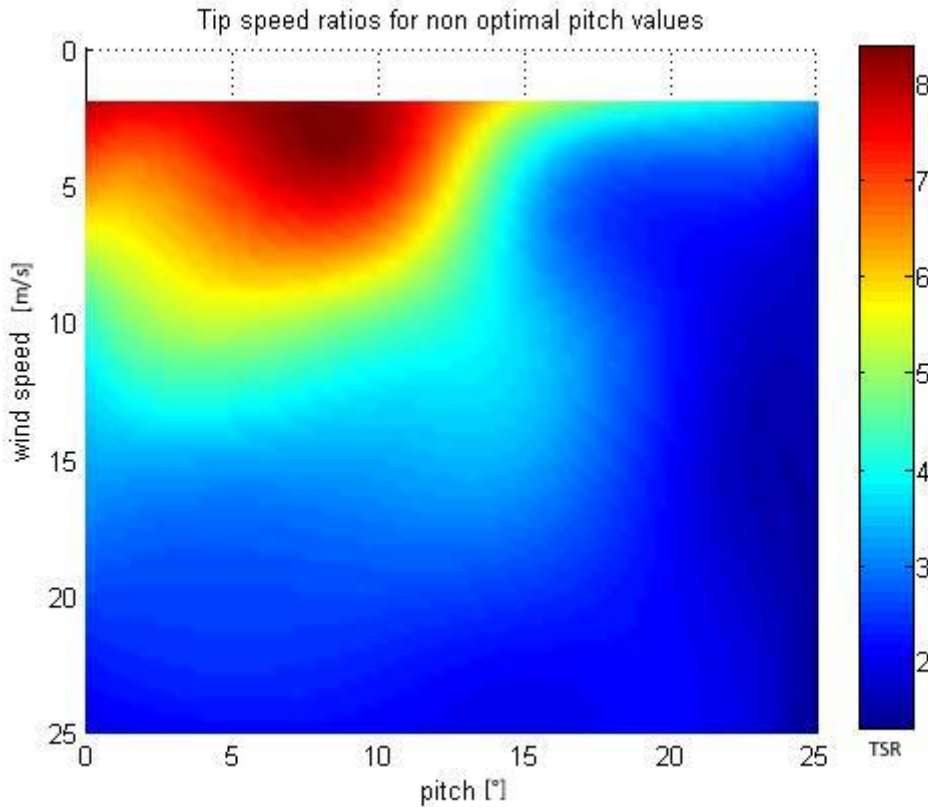


Figure 19 collected data is interpolated in MATLAB to create a continuous (and approximate) function for the entire range of blade pitch and wind speed scenarios. The data is based on the results from the ASHES NREL 5MW turbine simulations.

The data collected from the FEM analysis is used to predict the outcome of sub-optimal blade pitch settings in the turbine models.

### 5.1.3 Electro-mechanical models

The models above can be aggregated to express the power and torque output of the wind on the platform using Equation 6 and Equation 7 found in the sectioned entitled Theory 1.4 turbine theory.

For the purposes of this project the three 6 MW turbines are based on a scaled version of the NREL 5MW offshore turbine. The original data for the NREL 5MW turbine is open source material available to the research and development community. For in depth descriptions of this reference turbine see (NREL, 2009). Using Froude’s scaling laws a 6-MW reference turbine was developed by Scandinavian Wind in May of 2014. The data from this research is used in this report. The specifications of the scaled NREL 6-MW turbine can be found below in Table 8.

Table 8 specifications of the NREL 5-MW and 6-MW scaled turbines.

Property	Dimension (5-MW)	Dimension (6-MW)	Units
Hub height	87.6	110	m
Rotor diameter	126	154	m
Rated Power	5000	6000	kW
Rotor orientation/blade number	Upwind/3	Upwind/3	-
Rated speed cut-in/cut-out	2/25	2/25	m/s
Control	Variable speed/collective pitch	Variable speed/collective pitch	-

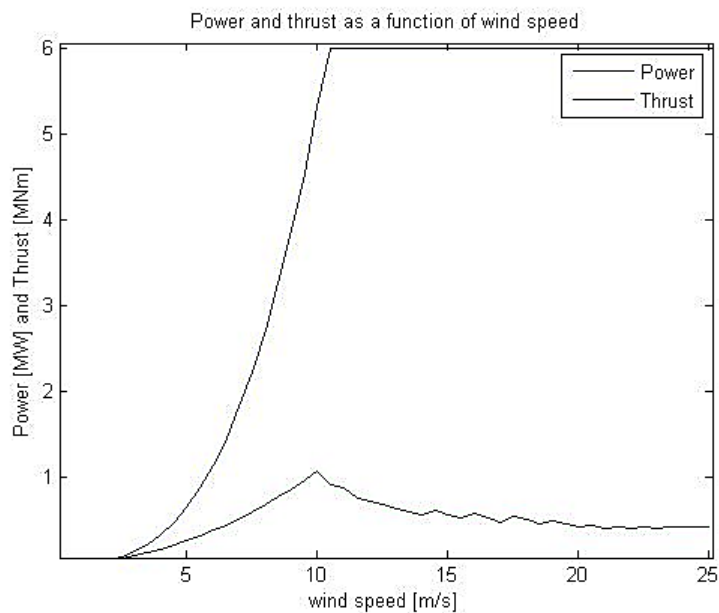
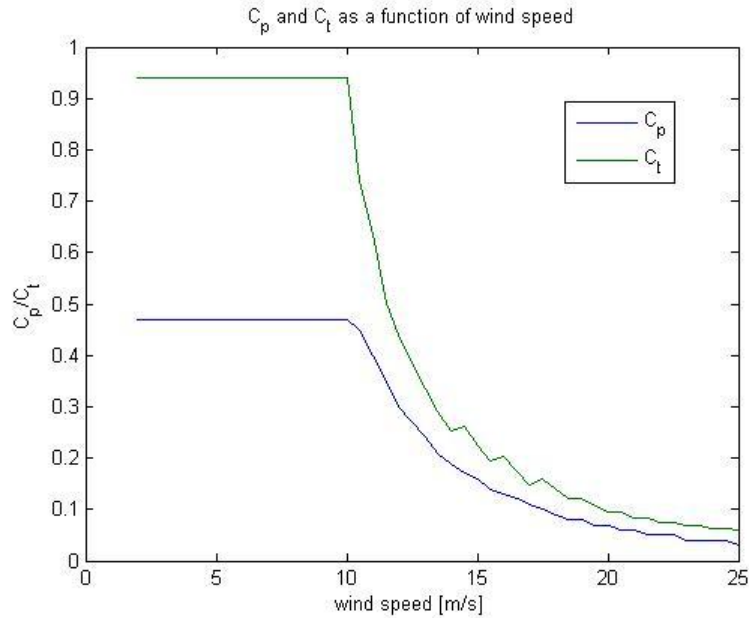


Figure 20 showing the power and thrust the turbine develops as a function of wind speed. The values are shown for normal (rated) blade pitch values of the NREL 6MW offshore wind turbine.

Figure 20 is particularly central to this work as the thrust generation is shown to peak at wind speeds around 10 m/s. From this diagram one can estimate that a single

turbine can produce at most, nearly 10 MN of torque to rotate the platform. Given the geometry of the platform, turbines 2 and 3 are then capable of producing around  $\pm 150$  MNm of torque for small wind angle deviations. While the platform does have a large moment of inertia, this torque value could theoretically accelerate the platform.



**Figure 21** because the turbine has a rated power of 6MW the power and thrust coefficients must be reduced (controlled through blade pitch) to limit the mechanical power being transferred to the generator as the wind speed increases. The data is shown for the NREL scaled 6MW offshore wind turbine.

The characteristic  $C_t$  and  $C_p$  values have been calculated for all blade pitch and TSR combinations (Scandinavian Wind, 2014:1). These values for the NREL 6-MW turbine can be seen below in Figure 22 and Figure 23. TSR (also denoted  $\lambda$ ) is defined as the relationship between the rotor speed and the free wind speed as follows:

**Equation 20**

$$TSR = \frac{\text{Tip speed of blade}}{\text{Wind speed}} = \frac{\omega R}{v} = \lambda$$

Where  $\omega$  is the angular velocity of the rotor,  $R$  is the radius of the turbine disc and  $v$  is the free wind speed.

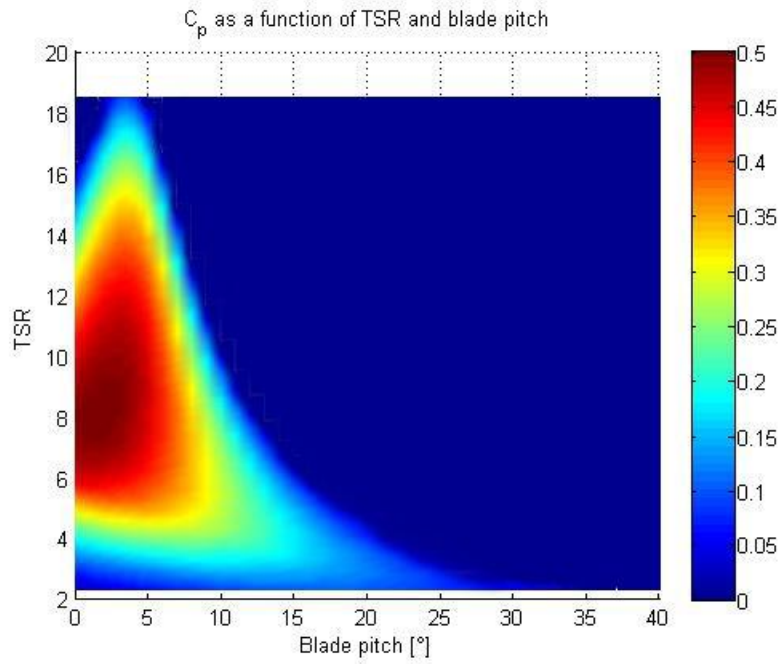


Figure 22 showing all known values of  $C_p$  for the scaled NREL 6-MW offshore wind turbine (Scandinavian Wind, 2014). The power coefficient is shown here as a function of turbine blade pitch and tip speed ratio.

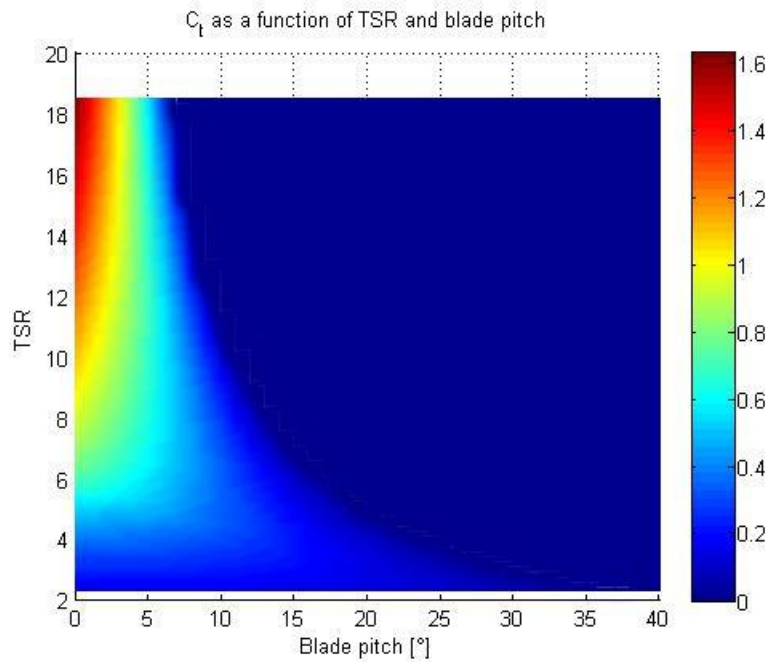


Figure 23 showing all known values of  $C_t$  for the scaled NREL 6-MW offshore wind turbine. (Scandinavian Wind, 2014) The thrust coefficient is shown here as a function of turbine blade pitch and tip speed ratio.

Combining the results of the NREL 6MW turbine study with the results of the wake and blade analysis, the electro-mechanical model can be visualized below in Figure 24

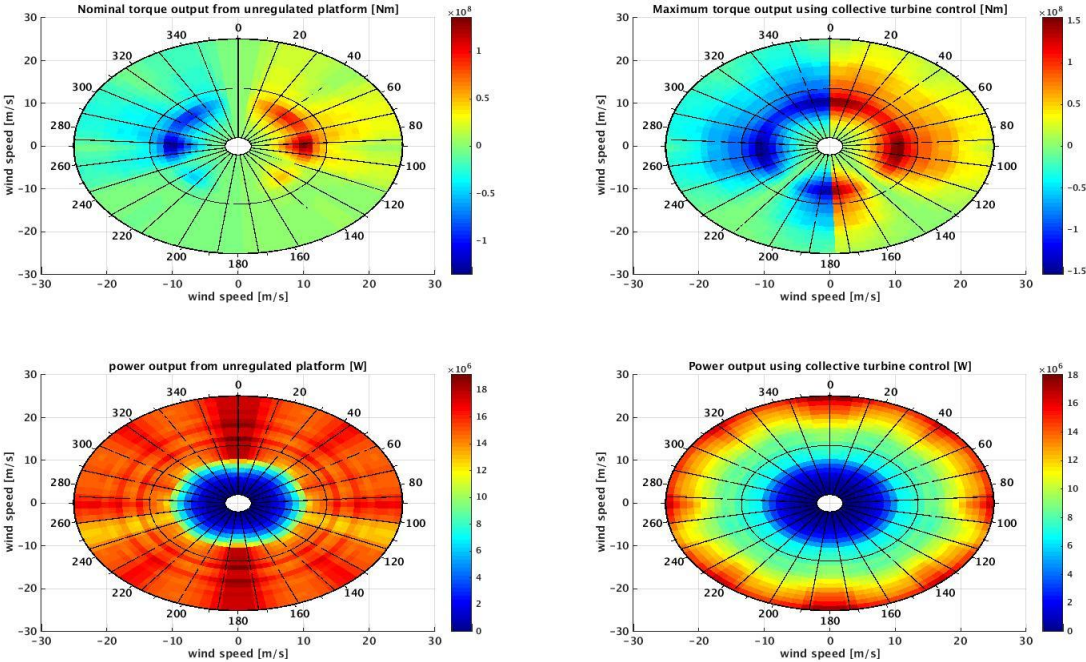


Figure 24 showing the results of the electro mechanical model. On the left, the turbine is shown unregulated, with nominal blade pitch values, representing a base line scenario. To the right the turbines are collectively regulated to produce maximum thrust on the H3-18MW platform. Torque and power values between these two extremes can be achieved, which should allow for good control of the platform in yaw.

Note in Figure 24 the manifestation of the wake analysis as a reduction in power and torque at specific wind angles. This follows as a result of Equation 6 and Equation 7 as well as Equation 8 (see section entitled Theory 1.3 wake theory). The wake model is most apparent around 40, 90 and 130 degrees (and corresponding angles over 180 degrees due to symmetry) as these angles represent a maximum turbine/wake interaction.

### 5.2 System identification

The PRBS signals are generated in MATLAB. Figure 25 and Figure 26 show the inputs/output from one such simulation. From the simulation results, a linear state space model is approximated using the theory expressed in Equation 10, Equation 11, Equation 12, and Equation 13.

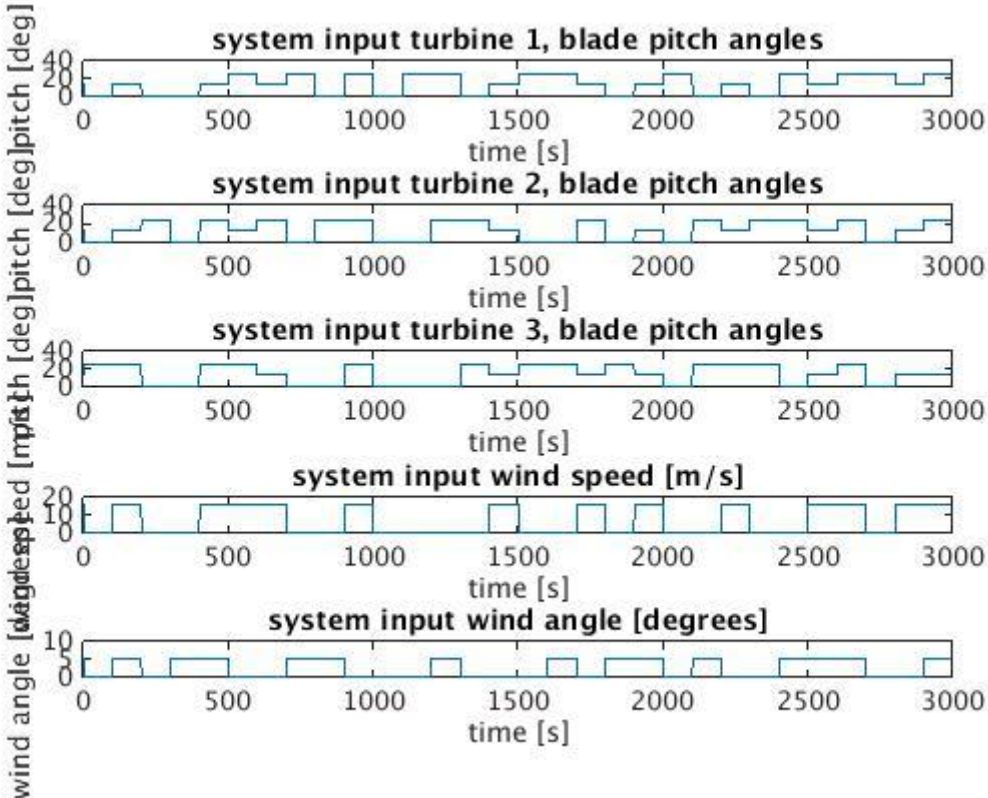


Figure 25 showing a sample of pseudo random binary signals (PRBS) inputs; wind speed, angle and the three blade pitch signals are shown for a 3000 second period. The signals contain low frequency information, and is sent into the simulator, creating a synthetic output used for system identification later.

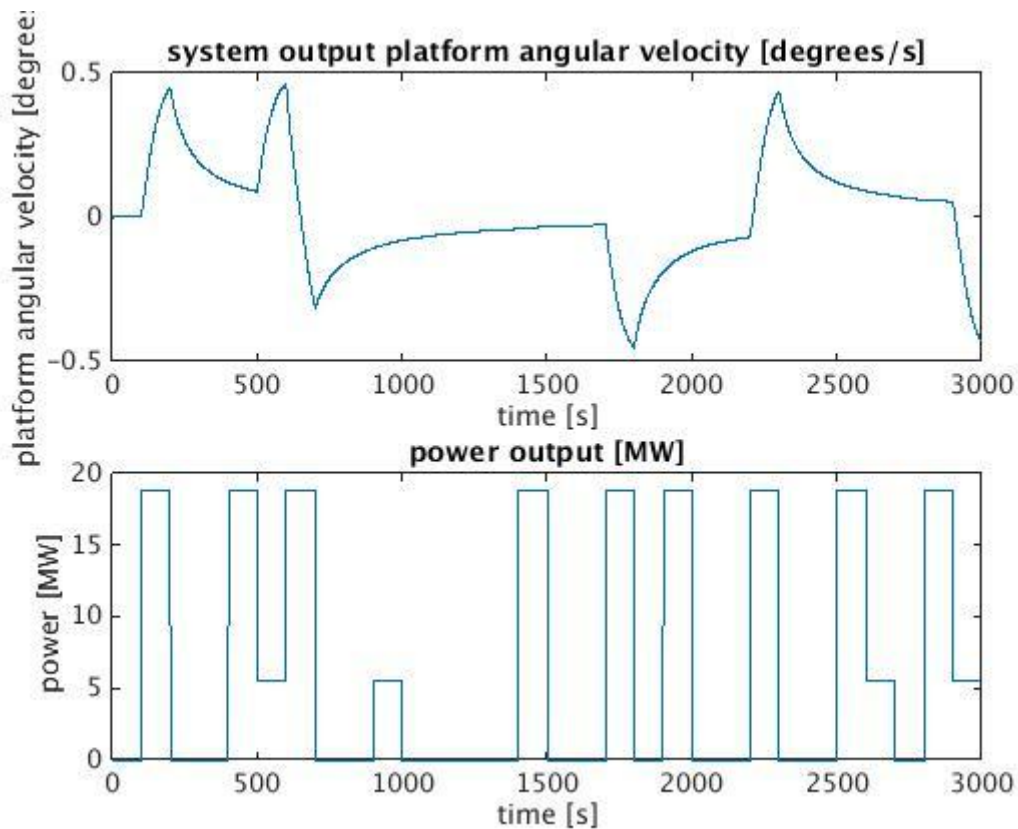


Figure 26 showing the output of the simulation. Fully understanding these figures is quite difficult given the complexity of the system and the number of contributing factors, however one can see the effects of wind speed and wind angle quite clearly. In reality the power output would be a smoother curve, given that the nacelle of the NREL 6MW offshore wind turbine has a maximum yaw velocity 5 degrees per second. This dynamic is lost here due to simplifications in the model.

From each of the scenarios (laid out in Method 1.2 model approximation) as seen in Table 5 a spectral model is approximated for comparison using the theory shown in Equation 10 to Equation 13 . Some of these models can be seen in Figure 27, Figure 28, and Figure 29 below. The results found in the spectral analysis give a hint as to how well the system will be approximated as a single linear system.



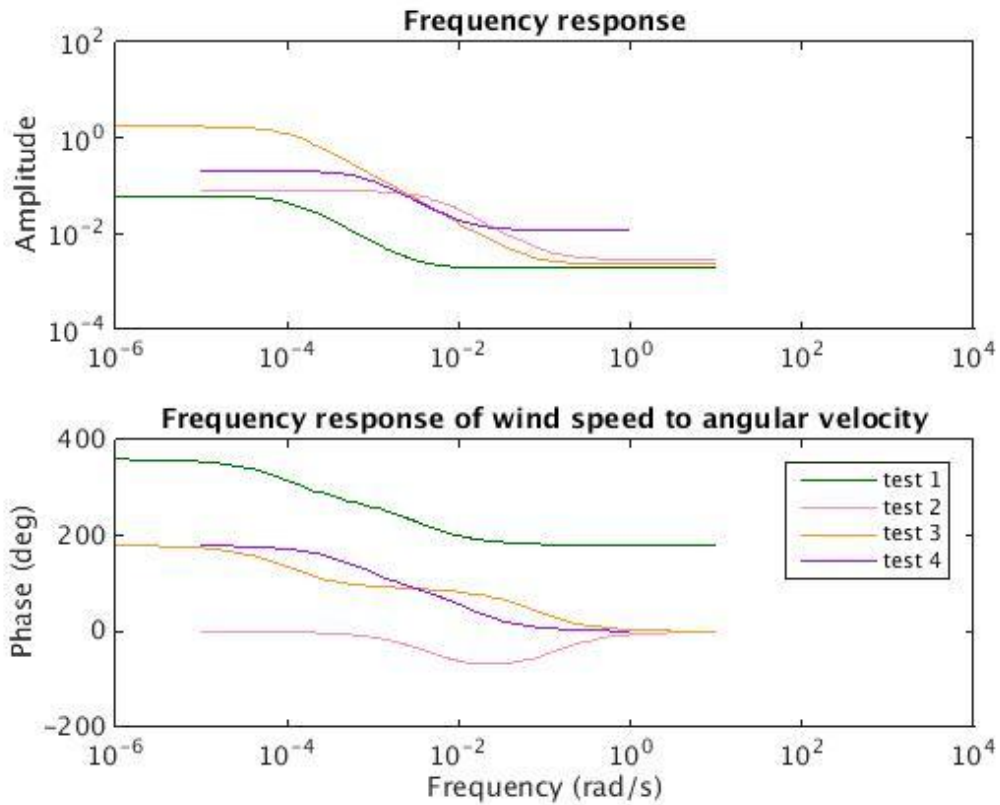


Figure 27 showing the simulated frequency response of the models describing wind speed to angular velocity. Each line represents the frequency response of a separate experiment. In each experiment, a maximum wind velocity, misalignment angle and/or blade pitch value was chosen. One such test is seen in Figure 25

From this figure the nonlinear behavior of the system can be seen as the deviation of the static gain and phase shift in the Bode diagram. The excitation frequencies of the system are however, generally grouped about the same frequencies, which may allow for a passable linear time invariant system approximation to be made.

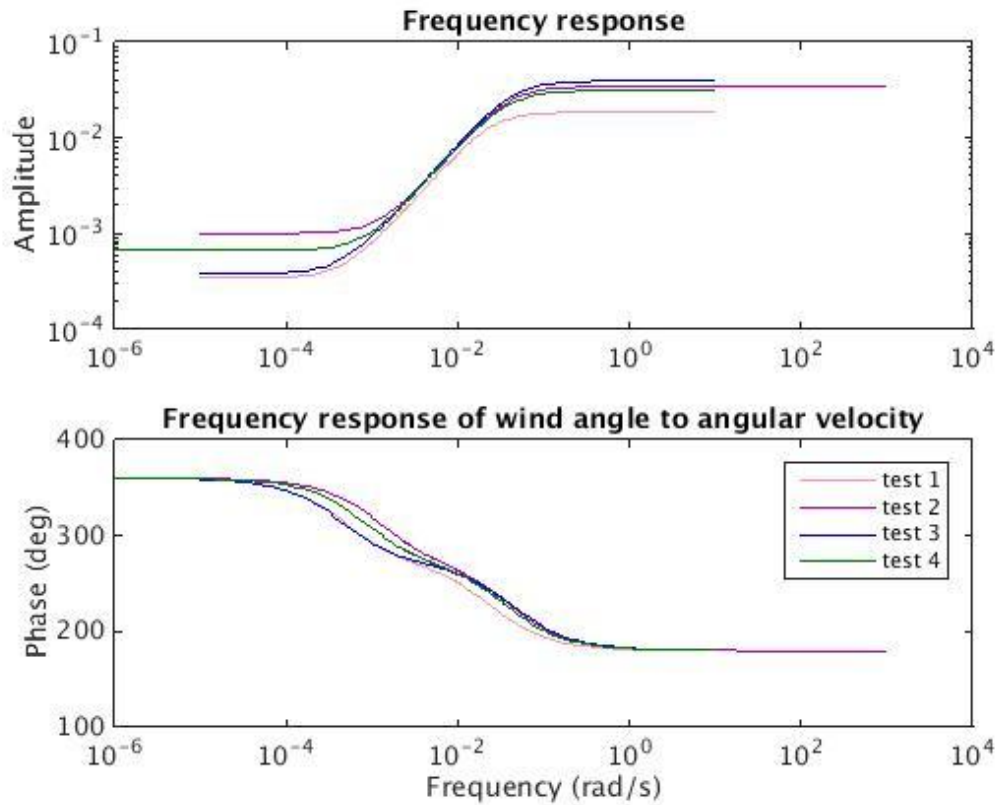


Figure 28 showing the simulated frequency response of the model describing wind angle to rotational velocity approximated from various data sets. Again, each line represents the frequency response of a separate experiment. In each experiment, a maximum wind velocity, misalignment angle and/or blade pitch value was chosen. One such test is seen in Figure 25

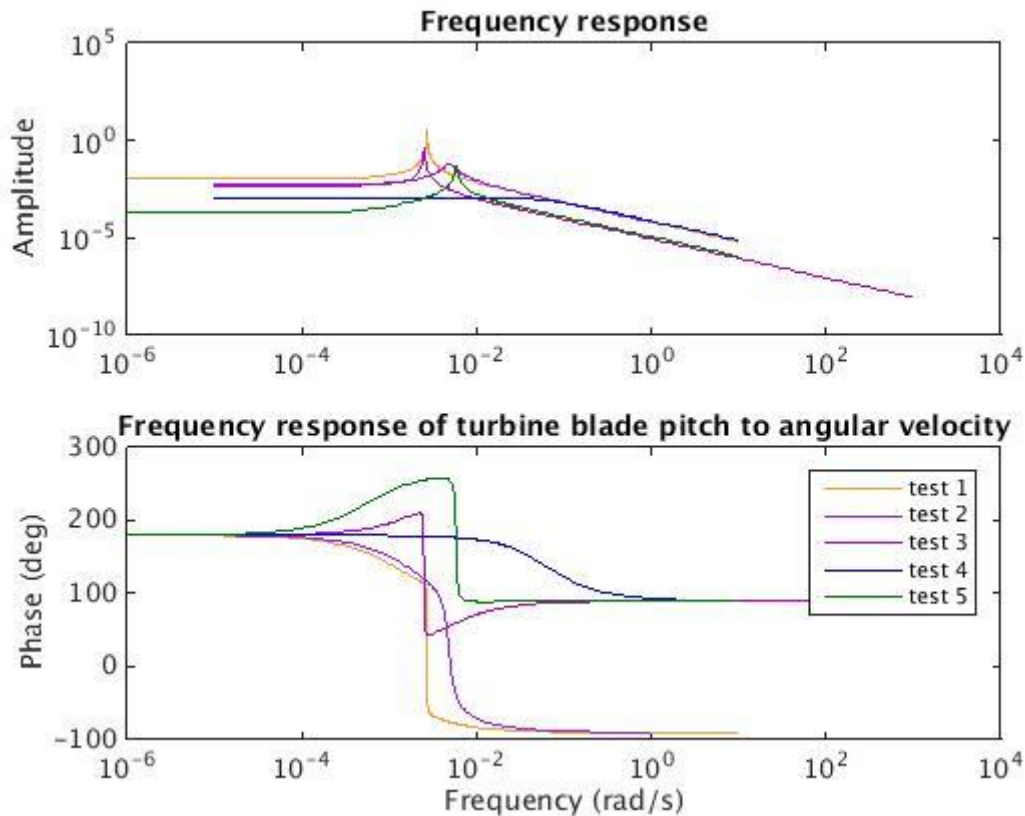


Figure 29 showing the frequency response between the input blade pitch of turbine 1 and the output of platform angular velocity. The grouping of the excitation frequencies are about the same point, however, differences in static gain may or may not allow for a linear approximation to be made.

Early attempts at constructing linear approximations of the true system from single data sets resulted in models with poor predictive ability during model validation. By *merging* the data sets in MATLAB's system identification toolbox (IDENT) from several (six different test) simulations, it is possible to adjust the approximated model for the differences in system behavior due to the nonlinear relationships. The model is approximated in IDENT using a nonlinear least squares method. This is an iterative process during which a linear model is refined in successive number of iterations, defined by the user. Though several methods of variable refinement are tested, model validation shows good fit to validation data when using a sub-space method called N4sid to identify parameters. The model is given as a transfer function with 5 inputs and 2 outputs.

This transfer function model is converted to an equivalent minimal realization state space model with 13 states. From this first approximation model, efforts are made to reduce the models complexity in MATLAB. It is often desirable (if possible) to reduce the order or number of states in any given model, especially for the purposes of systems control. (Schilders, et. al., 2008:26-8) By reducing the size (order) of the

model, control calculations become simpler, and solutions can be found faster. Similarly, it also shows that important behavior and attributes of the larger model can be preserved in a simpler way. Model reduction is performed here using predefined functions in MATLAB built on Hankel singular value criteria. This method allows one to reduce the order of the model without sacrificing key features. (Schilders, et. al., 2008:26-8) To test the reduced models against the original larger model, the validation simulation is shown in Figure 30 below. Note how the reduced model orders preserve the flavor of the more complex model, without offering too much in terms of accuracy.

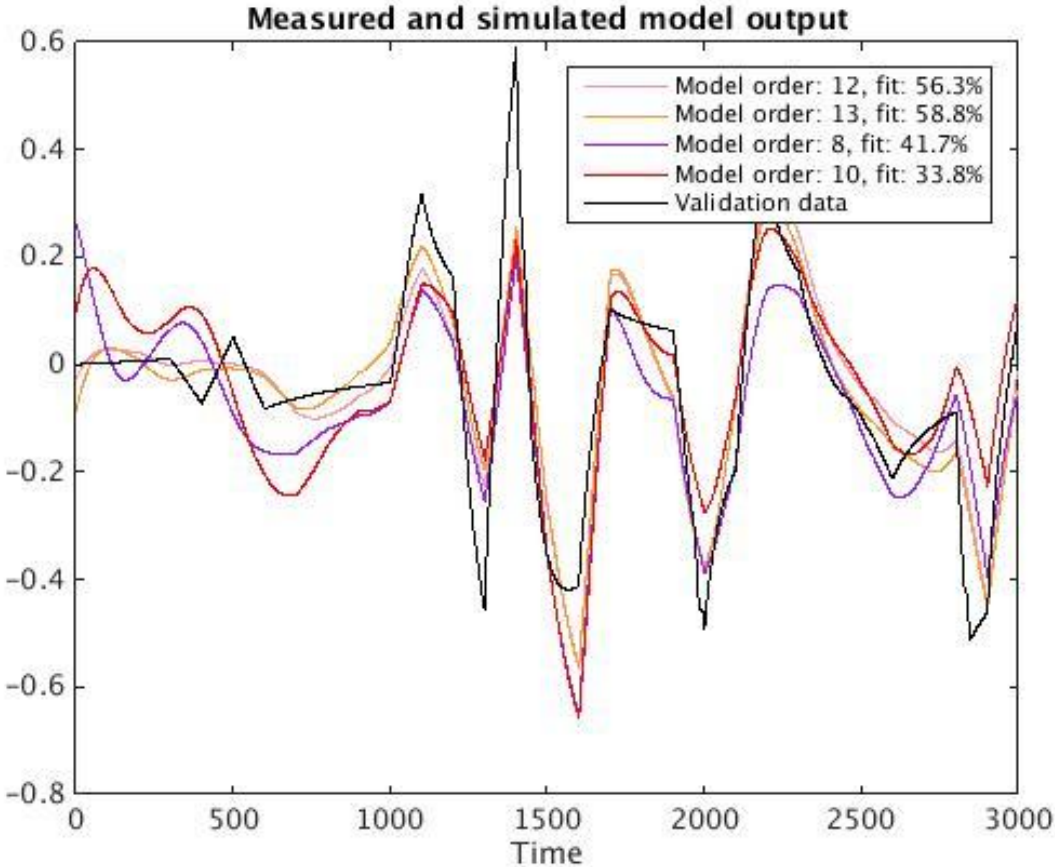


Figure 30 showing the simulated output of the main model and reduced counterparts as compared to validation data. The fit to estimation data percentage is nearly 70%. One can see however obvious signs of over fit, which reduces the predictive quality of the model.

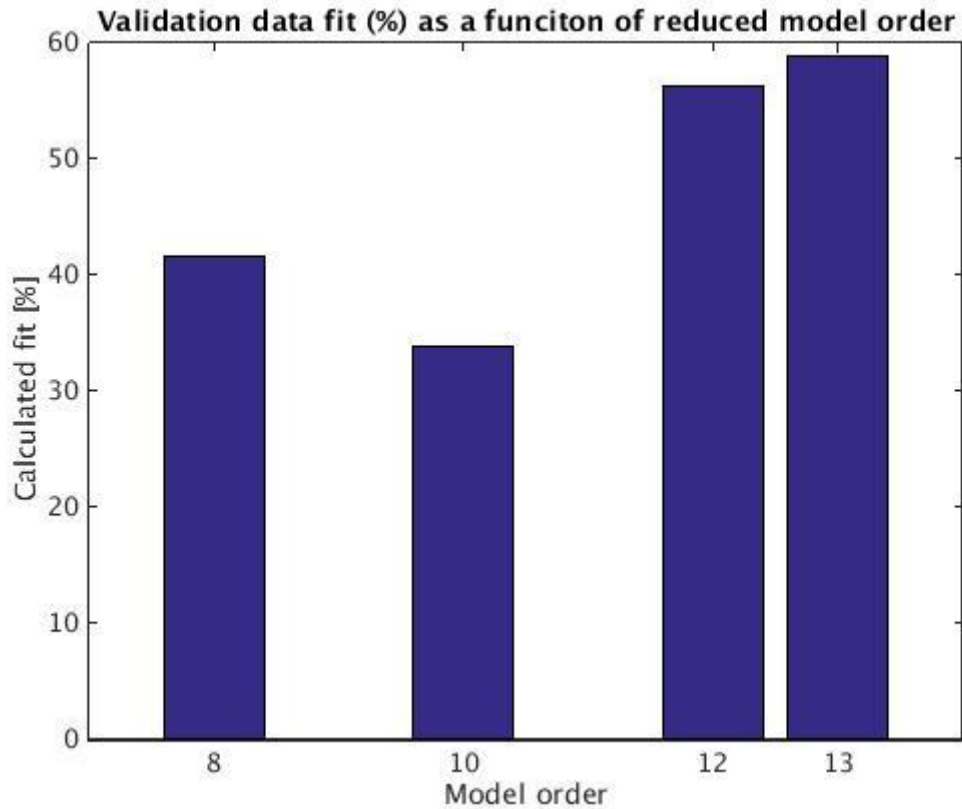


Figure 31 showing the fit to estimation data percentage as a function of chosen model order. This graph corresponds to the simulation in Figure 30. The original model has 13 states, and subsequent models are reduced using the Hankel singular value criteria.

The estimated transfer functions are converted into two state space models in MATLAB, one for platform angular velocity and one for power production. Both models use wind speed, wind angle and blade pitch angles for the three turbines as inputs. MATLAB analysis show that both models are minimal realizations, that is to say, both models are observable *and* controllable.

The resulting state space models are of the form shown below, and the coefficient matrices can be found in the appendix at the end of this report.

$$\dot{x} = Ax + Bu$$

$$y = Cx$$

Where  $x$  contains the states,  $u$  contains the inputs as follows:

$$u = \begin{pmatrix} \textit{wind speed [m/s]} \\ \textit{wind angle [^\circ]} \\ \textit{turbine 1, blade pitch [^\circ]} \\ \textit{turbine 2, blade pitch [^\circ]} \\ \textit{turbine 3, blade pitch [^\circ]} \end{pmatrix}$$

... and  $y$  is the output signal for each state space model (platform yaw velocity and power output) respectively. The platform yaw (angular) velocity has 15 states and the platform power output representation has 18 states. See appendix for coefficients.

### 5.3 System control

As previously explained in the section entitled Method 1.3 platform control, The SIMULINK based MPC regulator was found to contain system errors that have yet to be resolved in the available version. The results shown below are derived from a simpler, non-adaptive algorithm which calculates 'next-step' blade pitch signals based only on platform position relative wind. In other words, if the platform lags the wind, the blade pitch is increased such that the resulting torque on the platform is in the direction of the wind. These input signals are not calculated to be optimal, rather they are chosen to show how the platform *could* react to measured wind signals. To simulate this, the control schedule shown in Figure 9 is modified using the platform angle relative wind direction as the bang-bang criteria for blade pitch signals. The maximum pitch may not exceed 25 degrees, and the lower bound is determined by wind speed.

Scenario 1, features a constant measured wind speed of 15 m/s and a step change in wind direction from 0 to 15 degrees at the time of the simulations start. The pitch values are chosen by a crude bang-bang regulator to highlight the platform dynamics. Bang-bang is a simple control method whereby a signal is either on or off, in this case the pitch value is either maximized or minimized within the acceptable range. The pitch values chosen can be seen in Figure 32, note that these values are by no means optimal, they are chosen based on a simple criteria, in this case the platforms position relative the wind. When the platform lags the wind turbines 1 and 3 are told to increase blade pitch, causing a positive net torque, and vice versa as the platform leads the wind. The platform yaw resulting from this choice of pitch sequence can be seen in Figure 33 below.

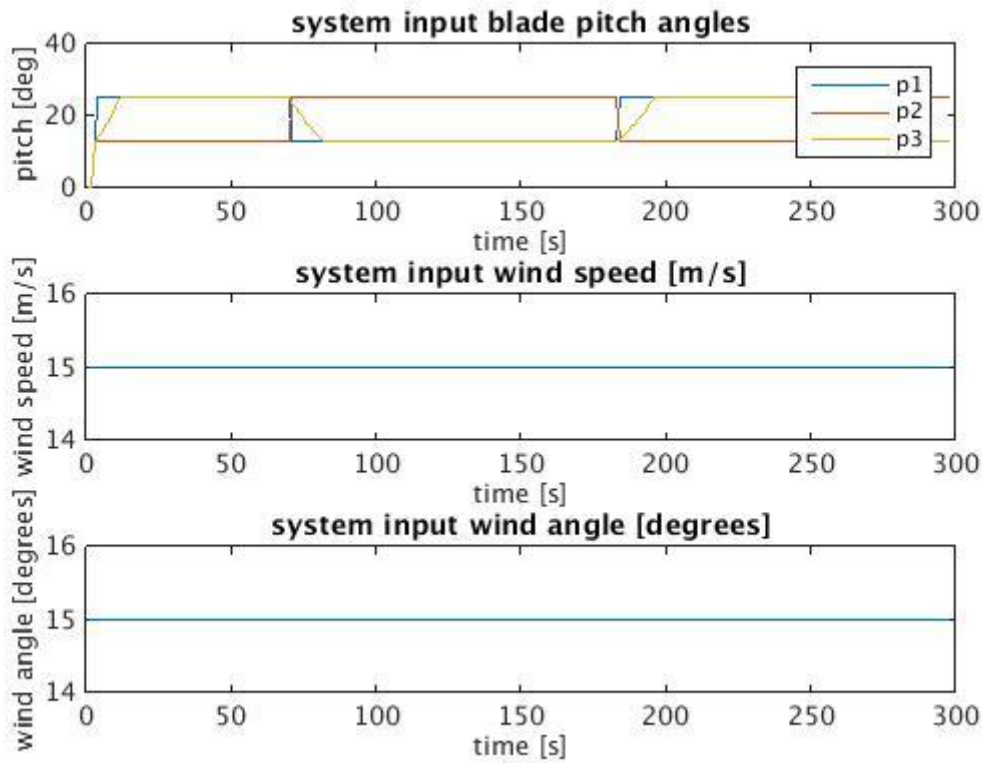


Figure 32 Scenario 1, showing the bang-bang regulated blade pitch values for turbines 1, 2 and 3 and the measured wind data. The legend shows the blade pitch angles for each turbine respectively. In this scenario the wind speed is a constant 15 m/s and the wind angle is a step of 15 degrees.



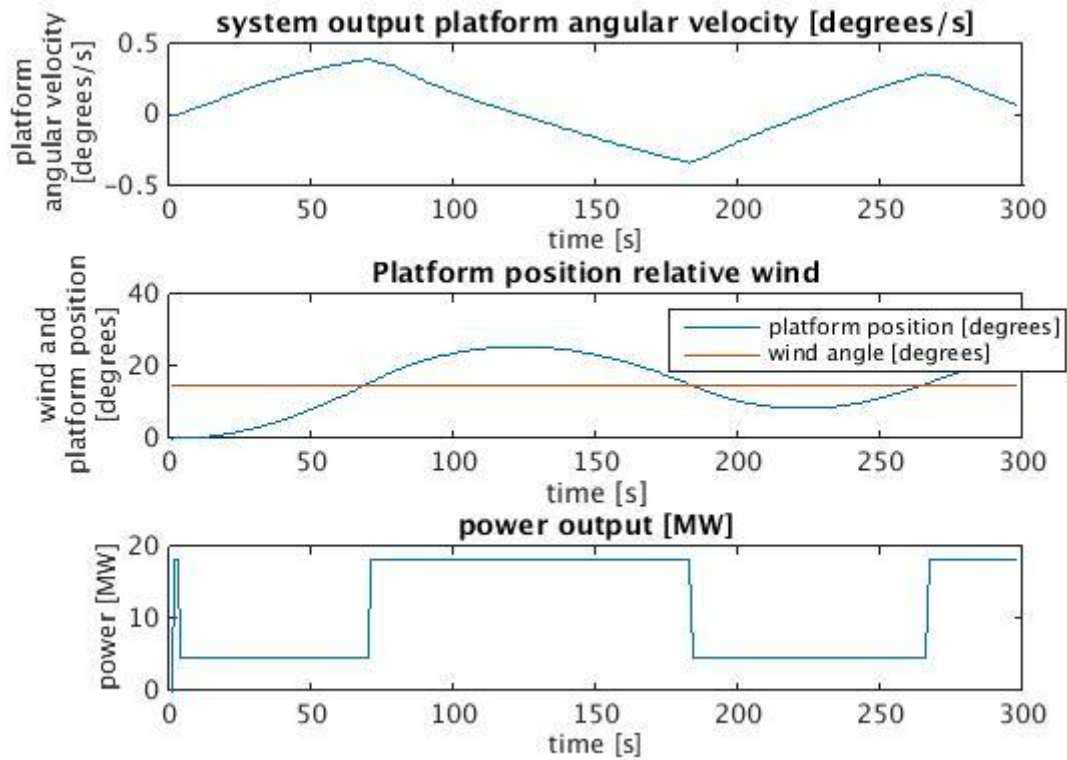


Figure 33 showing scenario 1, showing platform statistics during yaw. Note the large overshoot of the reference 15 degrees. This is due to poor choice of blade pitch values. The platform however has quick response and moves quite rapidly toward the 15 degree reference.

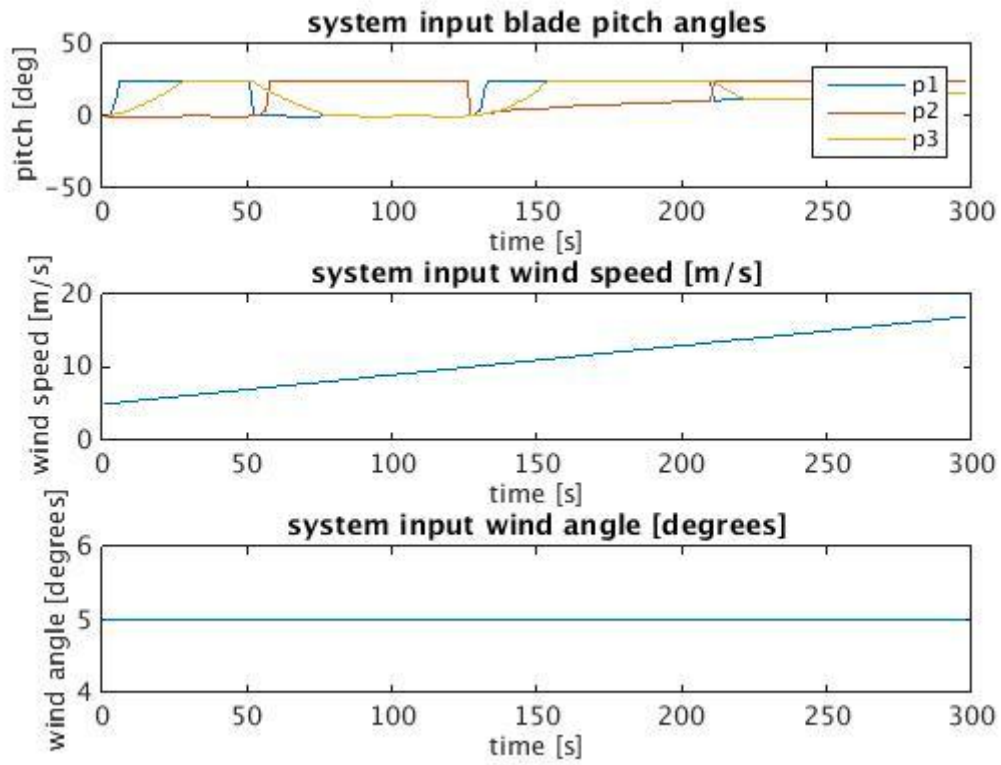


Figure 34 showing scenario 2. As the wind speed increases the lower bound for acceptable blade pitch values converges with the upper bound. The effects of this can be seen in Figure 35.

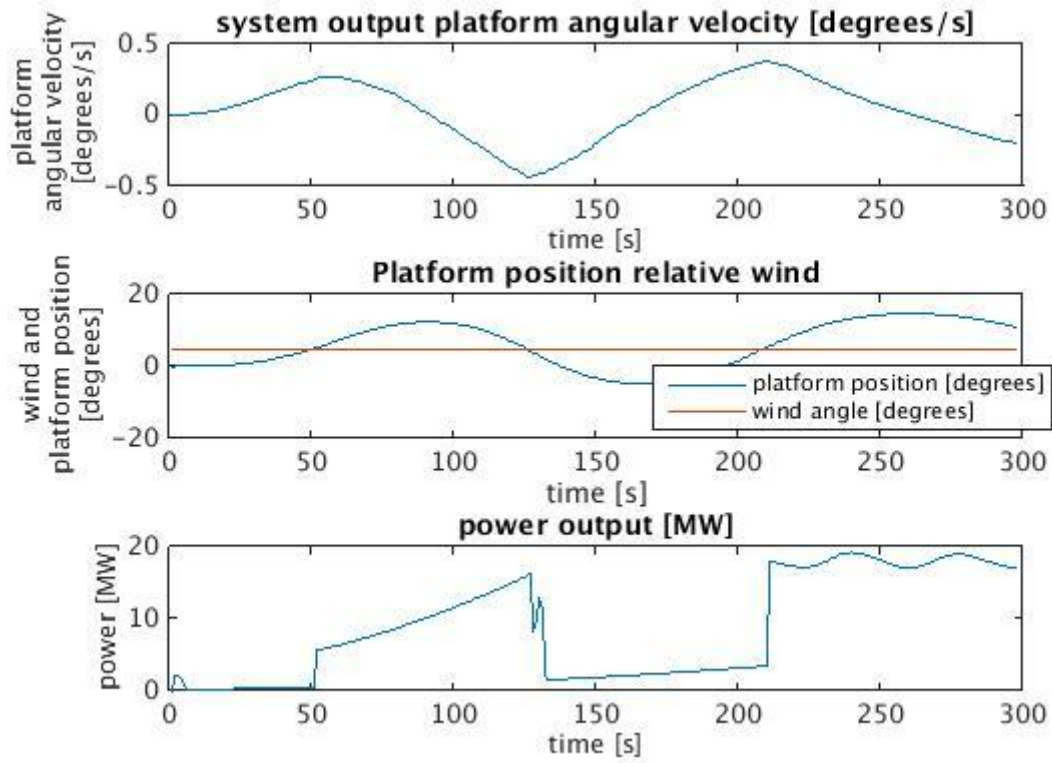


Figure 35 Results, scenario 2. Note that the platform reaction speed slows as the upper and lower blade pitch constraints converge. The platform however still shows relatively good speed in this region.

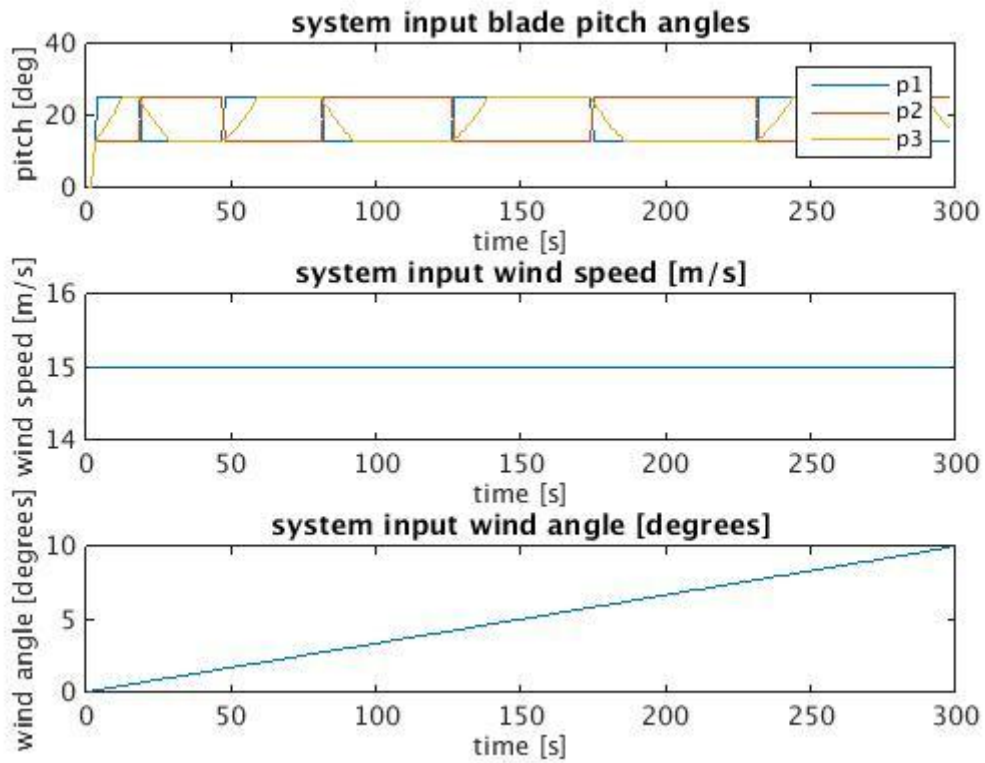


Figure 36 in scenario 3, the platform experiences a shift in wind direction that ramps continuously from 0 to 10 degrees. Because the wind speed is constant in this scenario, the turbine blade pitch can be chosen between the lower limit of 13 degrees and the upper limit of 25 degrees.

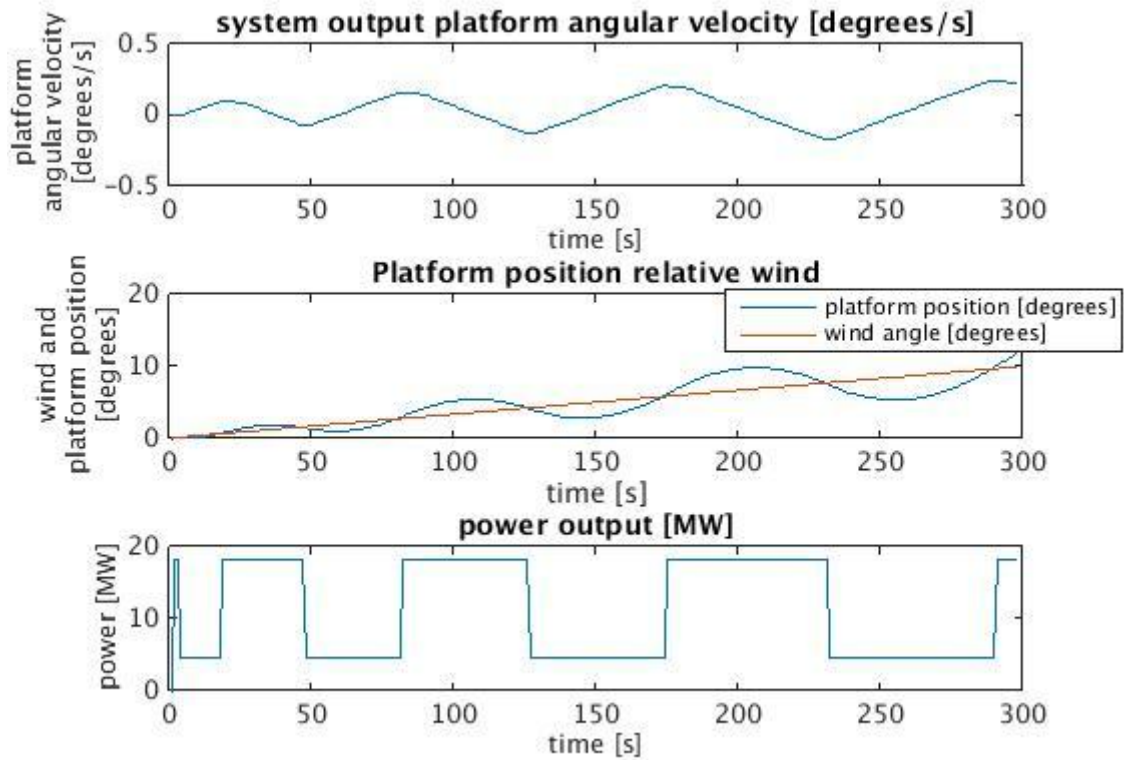


Figure 37 Results scenario 3. Note how the platform follows the wind direction. As the blade pitch values near optimal settings the power production approaches installed capacity. The platform can be driven to and from the wind direction, however as one sees near the end of the simulation, the regulator is ill suited to deal with this change in wind direction and the system becomes unstable.

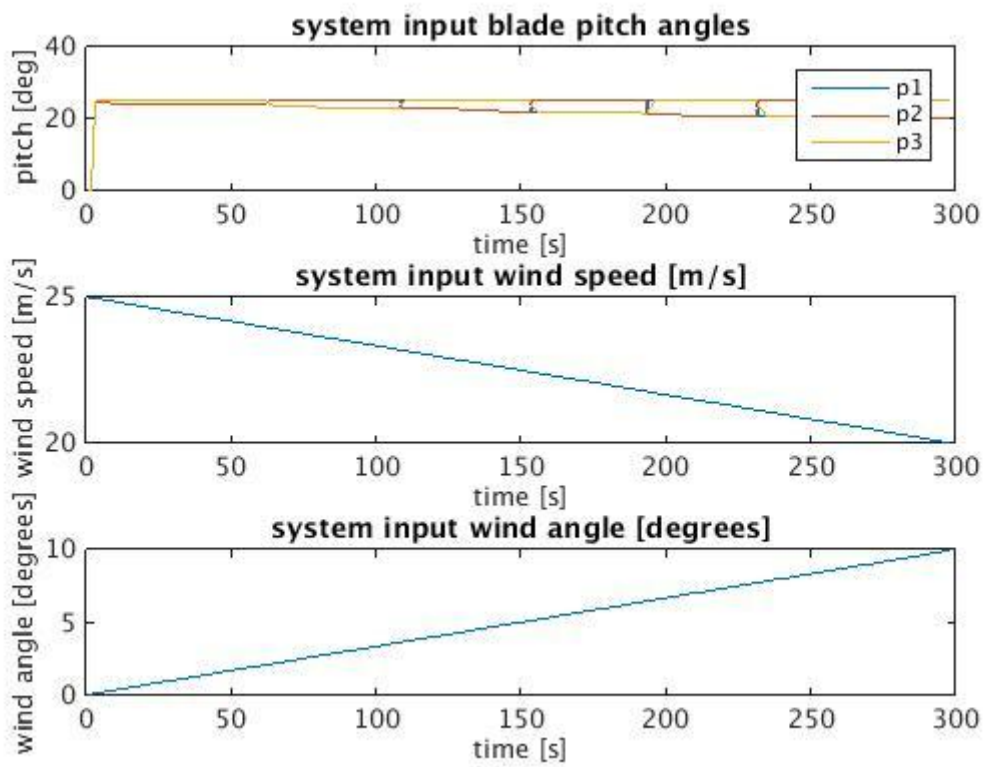


Figure 38 Scenario 4 inputs. In this scenario both the wind speed and wind direction ramp.

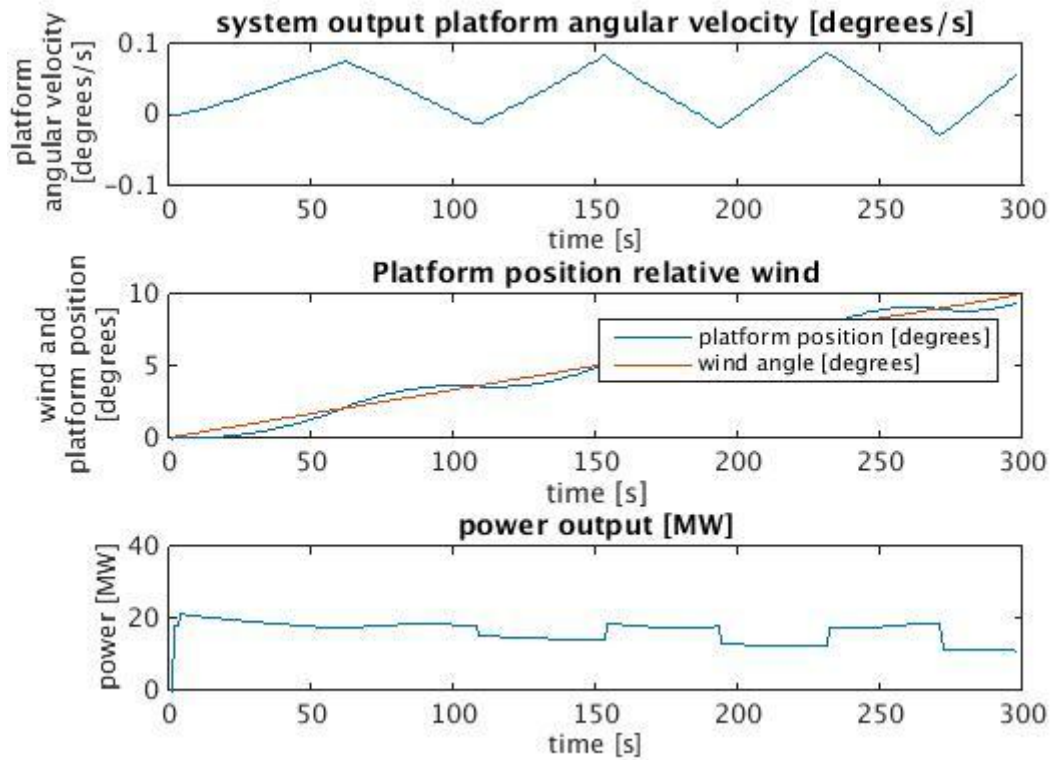


Figure 39 Results of scenario 4. Compare to results from scenario 3, note how the convergence of the upper and lower blade pitch bounds effect the platform response. The power production above 18 MW is most likely due to small errors in state-space model.

## 6 Sensitivity Analysis

While creating models, many calculations and assumptions concerning physical constants and properties were made. An obvious example of this is the H3-18MW platform's moment of inertia, used for solving the Morison equations. To calculate this number, sketches of the H3-18MW platform were studied, and measured by hand. Moreover assumptions of material density, thickness etc. were made. The resulting number ( $5.16e11$  [ $\text{kg}\cdot\text{m}^2$ ]) seems a reasonable order of magnitude, given the platform size. Despite this minor assurance, the platform moment of inertia is paramount in calculating the rotational velocity of the platform, and an analysis of the sensitivity of this value on the results is necessary. Likewise the assumed drag coefficient on the tubular steel structures was estimated (to 1.04 [-]) given review of relevant literature, however this value can vary greatly depending on type of steel, the surface smoothness, welding methods, etc. A simple sensitivity analysis showing how an increase/decrease in moment of inertia and/or drag coefficient effects the average and maximal rotational velocity and power is performed. In this analysis, data is collected first for a base line scenario, then for altered scenarios.

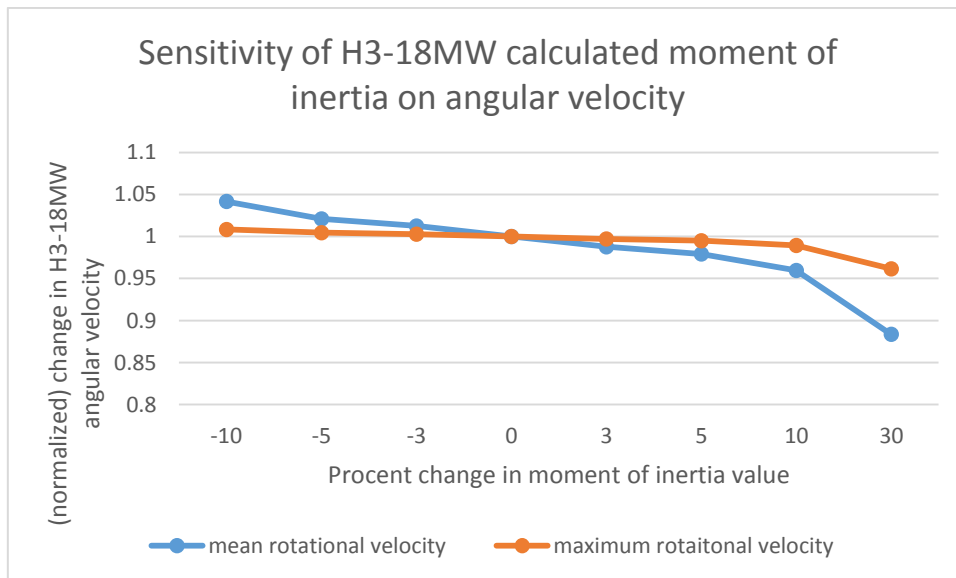


Figure 40 showing how angular velocity of the platform is affected by percentual changes in calculated inertial constant.



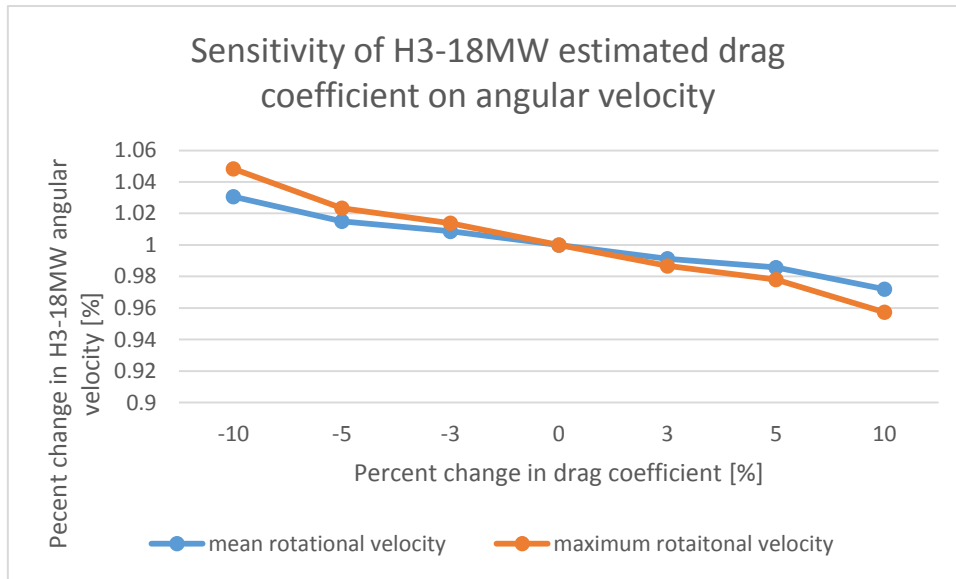


Figure 41 showing the results of the sensitivity analysis of drag coefficient on platform angular velocity.

The sensitivity of the rotational velocity to changes in platform moment of inertia and drag coefficient is noticeable, especially at the maximum  $\pm 10\%$  change in both parameters. Similarly, one sees that the average platform velocity is more sensitive in general to the calculated moment of inertia. A more advanced method of calculating moment of inertia would be advisable in the future, scale modeling would be advisable given the complex structure.

It can be said in general of this work that more advance methods of calculation would be advisable in future attempts at modeling and controlling the H3-18MW platform. However, as a feasibility study, the methods used here should give a generally good first insight into platform dynamics.

## 7 Discussion

It is unfortunate that it was not possible to demonstrate proper MPC control in this paper. The fact that a bang-bang regulator was used to compute blade pitch input signals instead of optimally calculated MPC control signals, does not however imply that an MPC controller cannot correct the platform heading. In fact- quite the opposite is true. Given a working MPC controller the platform heading can likely be corrected in a faster, far more optimal way than shown in the results above. The results presented here simply show that the platform *can* be controlled. In all the scenarios, the platform speed is reasonably fast even in scenarios 2 and 4 where blade pitch upper and lower limits converge. This suggests that even when the turbines are constricted by the blade pitch limit at higher wind speeds, the available torque (though diminished) is still capable of yawing the platform, albeit at a slower rate.

These results seem reasonable given the large amount of thrust available from each turbine, even at higher wind speeds. At suboptimal tip speed ratios, a large net torque can be exerted on the platform without pitching below the rated blade pitch angle. The power collected from the turbines is quite low during the yaw maneuvers. The bang-bang regulator does not consider the power output, merely the platform angle relative the wind. MPC controllers can be designed to optimize for several factors, and it is probable that with good MPC regulation, the power collected during yawing maneuvers would be higher than the results above suggest. That said, the reduction in power collection during maneuvers is still quite brief, even with bang-bang control.

The method described for dynamically positioning the H3 platform is novel in that the turbines are being used as the source of thrust. This concept has proved viable for the control of the H3-18MW platform, and has the potential to change the way engineers design wind parks in general. In reality however it may be difficult to modify turbine control schedules without consent (and aid) from manufacturers. Apart from the necessary partnership with manufacturers, modern turbine design and control is carefully overseen and regulated by external authorities such as the IPCC. In short, using the turbines on a floating platform as a thrust source for yawing maneuvers may be a difficult sell, see the section entitled ‘future works’ below.

The basic concept behind the control system described in this paper is grounded in an attempt to provide a *central* regulator with a predictive model of an *entire* wind park. Any wind park could be modeled in this way and regulators could be used to control a multitude of performance related variables including (but not limited to) park power output and turbine wake interaction. In traditional wind farms, turbines are placed in rows with turbine spacing calculated to provide maximum wind speed recovery from row to row in the event that wind direction deviates from a pre measured, standard direction. (Kusiak, 2010:685) Modern park layout optimization methods incorporate wake models, terrain limitations, and site specific wind distribution models to compute optimal turbine placement. (Kusiak, 2010:685) This is done to maximize the

potential wind energy recovery given a limited amount of space. This work would suggest that even with closely positioned turbines, power capture can be maximized and wake interaction minimized through what is essentially a multi turbine feedback system. Because an MPC regulator is able to predict how the turbines will behave collectively, the park layout becomes less dependent on physical space, relying instead on smarter control. Using this method wind parks could in theory economize on space to a greater extent than they currently do. Turbine thrust is utilized in order to control the H3 platform; however one may use the same technique to control the wind speed in the wake. In this way, turbines placed in rows experiencing heavy losses due to wake interaction could be made to operate at suboptimal tip speed ratios such that the average downwind speed in the created wakes is greater, and the total park output is higher. Indeed, with more advanced wake models, there is even potential to control the turbulence and increase component lifespan. The consequences of this could change the way wind farms are designed in a fundamental way; parks could contain more turbine units with good potential for greater turbine longevity in the same amount of space. While this technique is not used in practice, some attempts at controlling entire park production have been simulated (Johnson et al., 2009:44-62), (Steinbuch et al., 1988:237-246). Johnson has shown that a coordinated control of a two turbine park results in an increase in park output, using what she describes as a "...intelligent selection of operational set point(s)" (Johnson et al., 2009:44-62). Steinbuch et al. discusses a similarly promising result with a somewhat larger array though methods are only generally discussed. One might expect then, that this type of coordinated control for wind parks would be more commonplace, given that the technique was first described in the late 80's. In a historical context however, the research and development efforts in the wind industry has been primarily focused on turbine design (Pao et al., 2011:95-9). Since the 1980's hub height and turbine rotor diameter has increased steadily, see Figure 42. This trend is likely to continue until material limitations are met (Pao, et al., 2011:95-9).

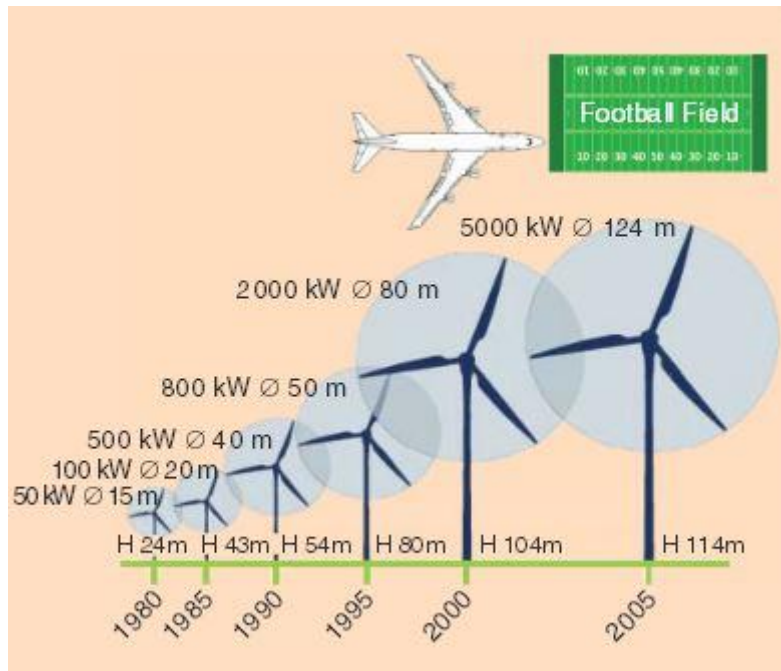


Figure 42 showing average turbine size increase from 1980 to 2005. Image adapted from Pao, et al 2011.

There exists however a growing community of engineers and turbine manufacturers that have started to withdraw support from the age old adage “bigger is better”. This is because the material costs and technical difficulties associated with futuristic mega turbines (10-20 MW) have a tendency to curb the economic viability of wind power systems. This is because the mass of the blades (in effect a measurement of turbine cost) increases as the cube of the blade length, while the gain in energy capture increases only as the square of the blade length. In other words, as turbines reach a maximum profitable size, the age old adage “bigger is better” may become “smarter is better”. It is the author’s opinion that during this phase in wind power innovation, solutions seeking to increase the profitability of wind power through more optimal control systems will begin to dominate the research and development sector.

Regardless of the techniques used to produce torque to yaw Hexicon platforms in the future, MPC control should be considered a powerful tool, capable of managing multiple task(s) in other situations. Theoretically this could be used to collectively control wind farms both on land and at sea. While the object of this thesis is to yaw a semi-submersible platform, the underlying idea of collective control in wind farms could be extrapolated to other areas of wind farm control. Wake interaction, park siting, and collective power production are all areas that this method may improve upon. This is an exciting new technique, of which (I believe) we have only seen the very beginnings of.

## **8 Conclusions**

### **8.1 Modeling**

The platform and turbine models contain many important physical relationships that should give a good first impression of platform dynamics. However, many of the methods used are simplifications of more complex theories and the large number of approximations may give a distorted image of the H3-18MW platform. It is important to note that while many of the simplifications are supported by theory, a more comprehensive analysis using FEM software and scale modeling will give a more conclusive result. The results obtained from the modeling process however seem to be of good quality, the platform does not behave in ways one would not expect, and given the geometry and mass of the platform, the speeds obtained in yawing maneuvers seem to be realistic.

### **8.2 System identification**

The system was approximated as a linear model using merged data sets in a black box fashion. This approach is not optimal given the nonlinear behavior/equations on which the system is based. The wake models and blade efficiency curves are very nonlinear and as a result, linear approximations are hard to achieve with black box methods. Looking at the results of the system identification as seen in Figure 30, the linear system can be interpreted as over-parameterized. This behavior disappears when applied to other validation data, (not presented in this report) instead seeming under-parameterized. This is due to the nonlinear behavior of the system. Future methods for improving a linear model of the system are presented in the section entitled future works, below.

### **8.3 Systems control**

From scenario 1 (Figure 33) we see that the platform has good speed and intention to reach the reference of 10 degrees. The regulator however is poorly equipped to handle the dynamics of the system and overshoot is imminent and highly apparent. Given long enough simulation time (30 minutes or so) however, the platform does eventually converge on 10 degrees. With a more adept regulator, one might expect that the platform would reach 10 degrees and settle there within 2 or 3 minutes.

Scenario 2 (Figure 34) is designed to show how the available torque changes as the wind speed increases. Though perhaps not very apparent, the platform reacts slower (decrease in angular acceleration) to the regulation as the wind speed increases. This is because the maximum net torque exerted on the platform decreases at higher wind speeds as seen in Figure 24.

Because the upper and lower available/allowed pitch values converge as the wind speed increases towards cut-out speed (see Figure 18), the available torque decreases in this area. While this is generally true, this behavior is most easily seen near zero

degrees at wind speeds approaching cut-out speed (25 m/s). Between rated speed and cut-out speed however there is still substantial amounts of torque being produced which allows for regulation, despite the blade pitch limitations.

Scenarios 3 and 4 are designed to showcase the platform reaction to slower changes in wind speed. As can be expected with bang-bang control, the results are somewhat erratic, however it is apparent that the platform is able to follow the wind at an acceptable angular velocity. Again, given proper MPC control, this is unlikely to occur; all models of the H3-18MW platform suggest good controllability.

While the platform experiences the largest angular accelerations near the rated wind speed, the positive acceleration produced during sub optimal blade pitch can be used to steer the platform to the desired location. Moreover, this acceleration increases as the platform nears the wind heading.

## 9 Future works

Simplifications and approximations were made during the course of this project which could have a significant impact on the reliability and precision of the designed controller in a real prototype H3-18MW platform. In this section, suggestions are made for possible follow up studies.

- For future works, MPC control is recommended as a control method. Given the amount of variables and constraints on the system, it should be a good way of optimizing yaw maneuvers.
- The hydrodynamics of the H3-18MW platform were simplified greatly using the Morrison equations as described in the section dealing with hydrodynamics. For a more accurate description of the platform, and its movement in a sea environment a detailed hydrodynamic study should be carried out using FEM software or scaled models. As previously explained the Morrison equations can be used for a first guess estimate of structures granted specific hydrological conditions. Structures well approximated by the Morrison equations are slim, compared to the wave length of the ocean environment. While much of the H3-18MW platform fits this description, some features (nodes etc.) may not be well approximated with the Morrison equations. FEM analysis will reveal the actual hydrodynamic coefficients of the H3 platform and provide information in more than one degree of freedom. For proper DP control of the platform information about platform movement in all degrees of freedom is necessary.
- The wake interference model may be expounded upon and a more detailed method could be used. Much in the same way the Morrison equations are a good first approximation for hydrodynamic features, the Jensen model is a good first approximation for aerodynamic features. However, because the platform's turbines are placed very closely 'near wake' effects will dominate and ideally, wake models which take into consideration the effects of rotating wake should be used as these forces dominate within the 2 turbine radius range (Renkema, 2007:7). Moreover, this paper assumes an absence of wind shear and turbulence.
- Turbine components are carefully designed to work in a very specific way. While it has not been investigated in this report, turbine design from a solid mechanics point of view must be considered as well. A more detailed analysis of the effects of sub-optimal turbine operation must be carried out to ensure safe operation throughout the lifetime of the turbine units. While some conclusions have been drawn from work with the FEM program Ashes, it is far from clear how turbines (and turbine blades in particular) will react to suboptimal tip speed ratios.

- The (linear state space) models presented in this work have been approximated using a grey box modeling method. While this has given some preliminary results and insight into the platform dynamics, it should be possible to express these relationships more explicitly in a white box model. It is suggested here that a more rigorous investigation of the H3-18MW platform dynamics be carried out to reveal a more accurate picture of the platform. This could lead to more optimal control, and for obvious reasons, more accurate results. The coefficients expressed in the state space models (as found in the Appendix) have not been shown with standard deviations (accuracies), as the results here are intrinsically uncertain. The model produced in this work is simply a first approximation, and while many aspects of the H3-18MW platform may be well represented, information is always lost in linear approximations of nonlinear systems.



## Bibliography

Adelaja, A., McKeown, C., Calnin, B., Hailu, Y. Assessing offshore wind potential. Energy Policy, Vol. 42, March 2012.

AMSOC. A report by the AMSOC committee on: Drilling thru the earth's crust. National academy of sciences, national research committee, September 1959.

Annoni, J., Seiler, P., Johnson, K., Fleming, P., Gebraad, P. Evaluating Wake Models for Wind Farm Control. American control conference June 2014.

Balchen, J., Jenssen, N., Mathisen, E., Sælid, S. A dynamic positioning system based on Kalmar filtering and optimal control. Modeling, identification and control, Vol 1, No. 3, pages (135-163) 1980.

Barthelmie, R., Folkerts, L., Larsen, G., Rados, K., Pryor, S., Frandsen, S., Lange, B., Schepers, G. Comparison of wake model simulations with offshore wind turbine wake profiles measured by sodar. Journal of atmospheric and oceanic technology, Vol. 23, 2005.

BlueH. Floating platform technology for offshore wind. <http://www.bluehgroup.com/>. Accessed August 2014.

Boyd, S. Lecture 16, Model Predictive Control. Convex optimization II, Stanford University. 2010. Accessed September 2014. <http://freevideolectures.com/Course/2289/Convex-Optimization-II/16#>

Butterfield, S., Musial, W., Jonkman, J., Sclavounos, P., Wayman, L. Engineering challenges for floating offshore wind turbines. NREL and MIT. Conference paper NREL/CP-500-38776. September 2007.

Chakrabarti, S. Handbook of offshore engineering, offshore structure analysis. First edition, 2005.

Chen, H., Wan, L., Wang, F., Zhang, G. Model predictive controller design for the dynamic positioning system of a semi-submersible platform. Journal of Marine Science, Volume 11, pages 361-376. 2012

Dosaev, M., Klimina, L., Lokshin, B., Selyutskiy, Y. Control systems for technological processes, on wind turbine blade design optimization. Journal of computer and system sciences international, Vol 23, No 3. Pages 402-409 Institute of mechanics of Lomonosov Moscow state university, January 2014.

Erlic, I., Shewerega, F., Feltes, C., Koch, W. F., Fortmann, J. Offshore windpower generation technologies. Vol. 101, No. 4 April 2013, Proceedings of the IEEE.

Esteban, D., Diez, J., López, J., Negro, V. Why offshore wind energy? *Renewable Energy*, Vol. 36, Issue 2. February 2011.

EWEA. The European offshore wind industry key 2011 trends and statistics. Published by EWEA, 2012. Accessed July 2014.

Finn, T. Hydroelasticity of a large floating wind turbine platform. Degree project in naval architecture, second level. KTH, Stockholm, Sweden. 2014.

GICON. Innovation in offshore wind power sector: The GICON SOF. <http://www.gicon.de/en/geschaeftsbereiche/gte/sof.html>. Accessed August 2014.

Grady, S., Hussaini, M., Abdullah, M. Placement of wind turbines using genetic algorithms. *Renewable energy*. Vol. 30, 2005.

Heidelberg, S. Wind turbines: fundamentals, techniques, application, economics. Chapter 17 (pages 615-652), *Offshore wind energy utilization*. 2006

J. Jonkman, S. Butterfield, W. Musial, G. Scott. Definition of a 5-MW reference wind turbine for offshore system development. Published by NREL, Feb 2009. Accessed July 2009. <http://www.nrel.gov/wind/pdfs/38060.pdf>

Johnson, K., and Thomas, N. Wind farm control: addressing the aerodynamic interaction among wind turbines. 2009 American Control Conference. June 10-12 2009. Pages 2104- 9.

Journée, J.M.J., Massie, W. *Offshore Hydrodynamics*, First edition. Delft University of technology, January 2001.

Kurian, V. Dynamic response of classic spar platforms subjected to long crested waves: Morison equation vs. diffraction theory. 2012 International Conference on Statistics in Science, Business and Engineering (ICSSBE), 2012

Kusiak, A., Song, Z. Design of wind farm layout for maximum wind energy capture. *Renewable Energy*, Vol. 35 issue 3. March 2010, pages 685-94.

Ladenburg, J. Attitude towards on-land and offshore wind power development in Denmark; choices of development strategy. *Renewable Energy*, Vol. 33, Issue 1, January 2008.

Lloyd's Register. Rules and regulations for the classification of a floating offshore installation at a fixed location. *Structural Design*, Part 4, Chapter 3 pages 5-10. April 2008.

Miller, D., Bishop, I. Visual assessment of off-shore wind turbines: The influence of distance, contrast, movement and social variables. *Renewable Energy*, Vol. 32, Issue, 5 April 2007.

NAOS. Project Mohole, commemorating the accomplishments of project Mohole. <http://www.nationalacademies.org/mohole.html>. 2011. Accessed August 2014.

Pao, L., Johnson, K. Control of wind turbines: approaches, challenges and recent developments. *IEEE control systems magazine*. March 16, 2011.

Renkema, D. Validation of wind turbine wake models- using wind farm data and wind tunnel measurements. Delft University of Technology. 2007

Roddier, D., Cermelli, C., Aubault, A., Weinstein, A. A floating foundation for offshore wind turbines. *Journal of renewable and sustainable energy*. Volume 2, Issue 3. 2010.

Shatto, H. History of dynamic positioning. DP committee of the marine technology society, 2011. <http://www.dynamic-positioning.com/history.html>. Accessed August 2014.

Schilders, W.H., van der Vorst, H.A., Rommes, J. Model order reduction, Theory, research aspects and applications. Springer publishing, 2008. Pages, 26-28.

Song, Z., Kusiak, A. Design of wind farm layout for maximum energy capture. *Renewable energy*, Vol. 35, 2010.

Sørensen, T., Nielsen, P., Thøgersen, M. Recalibrating Wind Turbine Wake Model Parameters – Validating the Wake Model Performance for Large Offshore Wind Farms. EMD international and EWEC, published 2006.

StatOil. Hywind by StatOil: the floating wind turbine. [http://www.statoil.com/en/TechnologyInnovation/NewEnergy/RenewablePowerProduction/Offshore/Hywind/Downloads/Hywind\\_nov\\_2012.pdf](http://www.statoil.com/en/TechnologyInnovation/NewEnergy/RenewablePowerProduction/Offshore/Hywind/Downloads/Hywind_nov_2012.pdf). Accessed August 2014.

Steinbuch, M. Boer, W., Bosgra, O., Peters, S., Ploeg, J. Optimal control of wind power plants. *Journal of wind engineering and industrial aerodynamics*, Volume 27. Pages 237-46. 1988.

Techet, A. Hydrodynamics and added mass. MIT department of mechanical engineering and center for ocean engineering. Readings, 2005. <http://ocw.mit.edu/courses/mechanical-engineering/2-016-hydrodynamics-13-012-fall-2005/readings/2005reading6.pdf>

Thomassen, P., Bruheim, P., Suja, L. A novel tool for FEM analysis of offshore wind turbines with innovative visualization techniques. *Proceedings of the twenty second*

(2012) international offshore and polar engineering conference. June 17-22 2012  
<http://www.isopec.org/publications/proceedings/ISOPE/ISOPE%202012/data/papers/vol1/2012-TPC-226Thoma.pdf>

Tong, W., Chowdhury, S., Messac, A. Impact of different wake models on the estimation of wind farm power generation. Aviation technology, integration and operations (ATIO) conference. 17/19<sup>th</sup> of September 2012.

Veselý, V., Rosinová, D. Model Predictive Control: Robust model predictive control design. Chapter 1, pages 1-5. August 18, 2010.

Windfloat pacific. Project information. <http://windfloatpacific.com/the-project/project-information/>. Accessed August 2014.

Wong, H.K.R., Schoukens, J., Godfrey, K.R. Design of multilevel signals for identifying the best linear approximation of nonlinear systems. IEEE transactions on instrumentation and measurement. Vol. 62, No. 2, February 2013.

Arwas, P. et al. Offshore wind cost reduction pathway study. Published by the Crown Estate, May 2012.

## Images

Dagher, H. Maine brings U.S. offshore wind dream to reality. <http://www.offshorewind.biz/2013/06/01/volturnus-18-launched-maine-brings-u-s-offshore-wind-dream-to-reality/>. Accessed August 2014.

Hexicon's H3-18MW. <http://www.hexicon.eu/offshore-platforms/h3-18mw.html>. Accessed July 2014.

Offshore floating platform types. DeepCwind tirelessly developing floating offshore wind. Renewableenergyworld. <http://www.renewableenergyworld.com/rea/news/article/2011/06/deepcwind-project-tirelessly-developing-floating-offshore-wind>. Accessed August 2014.

Water depth and distance to shore chart. EWEA, The European offshore wind industry key 2011 trends and statistics. Published January 2012. Accessed July 2014. [http://www.ewea.org/fileadmin/ewea\\_documents/documents/publications/statistics/EWEA\\_stats\\_offshore\\_2011\\_01.pdf](http://www.ewea.org/fileadmin/ewea_documents/documents/publications/statistics/EWEA_stats_offshore_2011_01.pdf)

MPC control. [http://en.wikipedia.org/wiki/Model\\_predictive\\_control](http://en.wikipedia.org/wiki/Model_predictive_control). Accessed December 2014.



$C = (-240.8 \quad -64.31 \quad 809.3 \quad -344 \quad 351.1 \quad 0.5955 \quad -42.87 \quad 227.5 \quad -231.5 \quad -87.06 \quad 437.6 \quad -114.1 \quad 103.6 \quad -9.589 \quad -143.8 \quad 88.72 \quad -64.87 \quad 19.26)$